OPTIMIZING PERFORMANCE OF MULTIPLE ACCESS MULTI-CARRIER MULTILEVEL FREQUENCY SHIFT KEYING SYSTEMS

TAY HAN SIONG

NATIONAL UNIVERSITY OF SINGAPORE

2005

OPTIMIZING PERFORMANCE OF MULTIPLE ACCESS MULTI-CARRIER MULTILEVEL FREQUENCY SHIFT KEYING SYSTEMS

TAY HAN SIONG

(B.Eng.(Hons.), NUS)

A THESIS SUBMITTED

FOR THE DEGREE OF MASTER OF ENGINEERING

DEPARTMENT OF ELECTRICAL AND COMPUTER ENGINEERING

NATIONAL UNIVERSITY OF SINGAPORE

2005

Acknowledgement

First of all, I'll like to thank my supervisors, Dr Chai Chin Choy and Professor Tjhung Tjeng Thiang, for all their generous advice and unwavering patience. This thesis will not be possible without their continuous support.

I'll also like to thank Mr Ng Khai Sheng and Mr Thomas Sushil. Their invaluable encouragement and friendship have put me through many rough times. This tenure has certainly been more rewarding due to the two of you.

Also to the Institute of Infocomm Research, for giving me the opportunity to conduct such exciting research.

Finally to my Mum and Dad for their endless support and understanding.

Table of Contents

Summary

The Multi-carrier Multilevel Frequency Shift Keying (MC-MFSK) system is a form of multi-tone MFSK systems, and it transmits on multiple frequency carriers simultaneously. The number of frequency-carriers used is termed the diversity order.

We derive a new analytical solution for the optimal diversity order of the multiple-access MC-MFSK system for achieving maximum throughput. The new formula relates the optimal frequency diversity order to the modulation level and number of users. We present numerically searched results for the optimal diversity order of MC-MFSK systems in both Rayleigh and Rician fading channels based on previously published works. We highlight that our formula gives very close results for optimal diversity order compared to the numerically-searched ones at SNR above 40dB. We also derive the optimal parameters for systems with several constraints such as error probability limit and restricted number of users.

For the first time, we also derive the steady state solution of the MC-MSFK system when control of the diversity orders is distributed to the users. We formulate the diversity control problem for two scenarios: 1) non-cooperative system users, where every user's objective is to maximize its own throughput, 2) cooperative system users, where every user's objective is to maximize overall system throughput. For each scenario, we present a steady state solution for the optimal diversity order. Using the concept of game theory, the solution in the first scenario corresponds to a Nash

equilibrium point but is Pareto inefficient, while the solution in the second scenario gives the desired Pareto efficient point.

Next we propose a method to select frequency-carriers in MC-MFSK systems to improve error performance. The method uses a combinatorial construction called Balanced Incomplete Block (BIB) Design to form selections of multiple frequency-carriers. With BIB design, any two selections will only coincide in at most one frequency-carrier. The selections are uniquely assigned to each symbol of every user, thus reducing the interference between the users in symbol transmission. We also present a selection process for optimal BIB design parameters. The performance of MC-MFSK systems using BIB design is compared to conventional MC-MFSK systems in Rayleigh channels. Our results show significant improvement for the proposed system for low number of user, while the performance is worse for larger number of users. Given a suitable user number, the method can be employed in MC-MFSK systems with the benefit of better error performance.

We also extend the MC-MSFK system to the Frequency-Hopping Multi-carrier (FHMC)-MFSK system by introducing additional frequency-hopping. We present an analysis for the frequency-time encoding techniques that provide maximum error performance. We show that the optimal frequency diversity order has the same relationship as the conventional MC-MFSK system, and is unaffected by the time-diversity. Hence the frequency-hopping, which improves error rate exponentially, can be used to achieve better error performance for the conventional MC-MFSK system.

Thus we show the versatility of the MC-MFSK system, along with its maximum capability in several practical conditions. We conclude that the MC-MFSK is a strong candidate for future spread-spectrum communication systems, which required high data rate and spectral efficiency.

List of Figures

List of Tables

Chapter 1

Introduction

In recent years, much research interest has been focused on multiple-access spread spectrum systems. This is due to the need for a new generation of communication systems, capable of delivering high data rate at wide bandwidth to mobile users. The system must also be spectrally efficient.

One of such candidates is the Multi-carrier Multilevel Frequency Shift Keying (MC-MFSK) system, which is proposed recently in [1,2] by Sinha as a candidate for future high-speed spread spectrum communication systems. The performance of this system is further analyzed for the Rician channel in [3] by Yu. It is a form of multi-tone MFSK system, and MC-MFSK systems transmit on multiple frequency carriers simultaneously. The system allows multiple-user access with its users sharing the same frequency and time space. These multiple users are differentiated by the unique permutations of frequency carriers, which each user uses to transmit its symbol. This system has several desirable properties such as frequency diversity and immunity to near-far effect. It also allows for an OFDM based multi-carrier implementation.

It is shown in [2] that the MC-MFSK system is able to achieve better performance than Goodman's frequency-hopping MFSK system. This motivated us to study the MC-MFSK system in greater depth. We discovered that the MC-MFSK system has the potential of delivering better performance, but so far, no research has been carried out to optimize its performance. In this thesis, our objective is to exploit the maximum

capability of the MC-MFSK system. Based on our results, the MC-MFSK system is presented as a strong candidate for future spread-spectrum communication systems.

In MC-MFSK systems, the number of frequency-carriers used per symbol transmission is termed the diversity order L. Along with the modulation level M, they are the main parameters in the MC-MFSK system. Throughout this thesis, we optimize the system with respect to these two parameters. In addition, we derive optimal parameters for the system under several system constraints such as error probability limit and fixed number of users.

We also optimize the MC-MFSK system when control of the diversity orders is distributed to the users. In this case, the diversity control problem is formulated for two scenarios: 1) non-cooperative system users, where every user's objective is to maximize its own throughput without any regard to other users. 2) cooperative system users, where every user's objective is to maximize the overall system throughput.

Next we propose a novel method of selecting the multiple sub-channels used by all users for symbol transmission. The selection of sub-channels improves the error performance of the multiple-access MC-MFSK system by reducing the degree of interference between the users. This method uses a combinatorial construction called Balanced Incomplete Block (BIB) design to form a collection of sub-channels selections, where any two selections will coincide in at most one sub-channel. These selections of sub-channels are uniquely assigned to each symbol of every user. Thus on symbol transmission, the effect of multiple-access interference is reduced.

Lastly, we extend the conventional MC-MFSK system to the Frequency-Hopping MC-MFSK system by introducing additional frequency-hopping to every user. In this system, each symbol transmission will span over several time hops and a different permutation of sub-channels will be used per hop. We analyze the error performance of this frequency-hopping MC-MFSK system, and optimize the system throughput with respect to the diversity order.

1.1 Literature Review

The MC-MFSK system is first introduced by Sinha in [1]. The MC-MFSK system is a multiple-access system based on OFDM implementation [1]. By making use of advances in OFDM technologies, the system can be easily implemented with the IFFT/FFT operations, which eliminate the need for banks of oscillators [4]. The MC-MFSK system has some advantages over both FH-MFSK and conventional Direct-Sequence (DS)-CDMA systems as follows. Firstly, compared to FH-MFSK system, the MC-MFSK system is more robust against the effect of large delay spreads as it has a lower signaling rate on individual sub-channels. Secondly, the DS-CDMA system is highly susceptible to the near-far effect [5] while the MC-MSFK system is immune to this effect. Thirdly, the MC-MFSK system achieves frequency diversity. Due to these advantages, Sinha et al. propose the MC-MFSK system as a strong candidate for future high-speed wireless system [1].

In [2], Sinha presents a derivation for the error performance of the MC-MFSK system. The main assumptions made in this evaluation are: 1) the system is under a Rayleigh fading channel, and 2) all its users have the same diversity order. The derived upper-bound for the symbol error rate of the system can be found in [2].

Using this expression, Sinha proves that the MC-MFSK system achieves a higher user capacity than conventional FH-MFSK systems. The expression is also shown to be an effective upper-bound for the error probability, with the bound been tighter for higher SNR. However, the proposed expression is mathematically complicated. The results in [2] show that there exists an optimal diversity order, which maximizes the MC-MFSK system performance. However, no further attempt has been made to evaluate this optimal diversity order analytically.

Yu et al. [3] evaluate the error performance of MC-MFSK systems for Rician fading channels. For a Rician channel, the authors use a novel approach of combining the line-of-sight (LOS) carriers of the multiple signals into a single LOS carrier, and combining the multipath components of multiple signals with other Gaussian noises to form a single Gaussian process. Hence, the probability density function (pdf) for the output of envelope detectors in MC-MFSK systems is first derived. This pdf is then used to evaluate of the false alarm and deletion probability of the tones in MC-MFSK systems. The false alarm refers to erroneous detection of a tone when none is actually sent, while deletion refers to failure to detect a tone when it is actually sent. Applying these probabilities using Sinha's analysis in [2], they derive the upper-bound for the error probability of the system. The difference between Sinha and Yu's analysis is in the expression for the false alarm and deletion probabilities. Therefore the error performance expression in [3] for the Rician channel is also as mathematically complicated as its counterpart in [2] for the Rayleigh channel. Similar to Sinha's analysis in [2], an optimal diversity order is also observed in [3]. Again no effort has been taken to optimize the performance of the MC-MFSK system.

In [6], Atkin et al. propose to use a combinatorial construction, called Balance Incomplete Block (BIB) design, for selection of frequency carriers in multi-tone MFSK modulation. Multi-tone (MT)-MFSK systems are an extension of basic MFSK systems, where the MT-MFSK system utilizes a permutation of frequency carriers for signaling instead of one carrier in basic MFSK systems. The authors in [6] use the BIB design to form the permutations of the frequency carriers. The interesting attribute of the BIB design is that the permutations will overlap on at most λ carriers, where λ is a user-defined parameter in BIB design. The authors show that the system using BIB design achieves a better performance than other MT-MFSK systems using designs such as Hadamard matrices. As for more details on the BIB design, we advise readers to refer to the works in [7] and [8].

The MC-MFSK system is evolved from the multiple-access Frequency Hopping (FH)-MFSK system proposed by Goodman et al. in [9]. In this thesis, the term FH-MFSK system refers to Goodman's system in [9]. The FH-MFSK system is different from the conventional FH spread spectrum system [10-12] as follows. In FH-MFSK systems, there is no segregation of bandwidth into sub-bands and the entire bandwidth is made up of M orthogonal sub-channels, where M is also the modulation level of the system. As for conventional FH spread spectrum systems, the entire system bandwidth B is segregated into multiple sub-bands each of M orthogonal sub-channels. To transmit a symbol m in the FH-MFSK system, the frequency-hopping sequence is generated by cyclic-shifting the user's hop-address by the value m. Since the pioneering work of [9], the FH-MFSK system has been studied by several researchers and it has been shown to offer a higher capacity than its conventional counterpart [13,14].

1.2 Thesis Overview

In Chapter 2, we describe the MC-MFSK system model. The decoding process of the system is explained. We also present derivations of the MC-MFSK system capacity and system throughput.

In Chapter 3, we derive a mathematically simpler expression for the error probability of the MC-MFSK system, by assuming that the channel is non-fading and of high SNR. We make use of this expression to derive a new analytical solution for the optimal diversity order, which maximizes throughput and minimizes error probability. By comparing it with the numerical results from previous works in [2,3], we verify that the optimal diversity order is valid for fading channels at SNR above 40 dB. By using our error probability expression again, we maximize the throughput of the MC-MFSK system under the constraints of an error probability limit and constant number of users. We also maximize the user capacity for the MC-MFSK system constrained by an error probability limit.

For Chapter 4, we study the diversity control problem in the MC-MFSK system when control of the diversity orders is distributed to each user. We formulate the objective functions for two different scenarios: 1) system users are non-cooperative and each user's objective is to maximize its own throughput; 2) system users are cooperative and their objective is to maximize the total system throughput. We then derive a new steady state expression for the solution of optimal diversity in each case. The solutions are then explained using game theory.

Next, in Chapter 5, we propose a method of sub-channels selection based on a combinatorial construction called Balanced Incomplete Block (BIB) design in MC-MFSK systems. The method improves the MC-MFSK error performance by limiting the overlapping of selected sub-channels between any two users to at most a single sub-channel. We will also introduce the properties of the BIB design and describe its deployment into MC-MFSK systems for our method of sub-channels selection. We derive the error probability and user capacity of the system, and use these derivations to analyze the effect of various BIB design parameters. Based on our analysis on the parameters, we also propose a method in selecting a suitable parameter pair for BIB design, which will maximize the error performance of the system. We will simulate and compare the performances of both MC-MFSK systems using our proposed method and conventional MC-MFSK systems.

In Chapter 6, we extend the MC-MFSK system to the Frequency-Hopping Multi-carrier (FHMC)-MFSK system. This is achieved by introducing additional frequency-hopping to the MC-MFSK system. Frequency-time code is needed for the system to select the permutation of frequency sub-channels at different time-hops. Thus we examine all practical forms of the frequency-time code, the distribution of their correlations, as well as their implementations. Using the same approach as in Chapter 3, we derive the error probability, bandwidth and optimal frequency diversity order of the FHMC-MFSK system. Based on these derivations, we also study the effect of system parameters such as time diversity, frequency diversity and modulation level, on the system measures like error probability and bandwidth. Finally we conclude the thesis in Chapter 7.

Chapter 2

Multi-Carrier MFSK System Model

The MC-MFSK system is adapted from a multiple-access Frequency-Hopping MFSK (FH-MFSK) system proposed by Goodman in [9]. The MC-MFSK system uses address code to generate a permutation of frequency-carriers for each symbol. A tone is sent simultaneously on each of the selected carriers for a given symbol duration. The system is also viewed as a special case of the Multi-tone Frequency-Hopping MFSK system [15,16] when the time diversity equals to unity.

2.1 Transmitter and Receiver

In the MC-MFSK system, the total bandwidth is divided into M sub-channels, each with an orthogonal carrier frequency like the MFSK system in [9]. $M=2^k$ is also the modulation level of the data, where k is the number of bits per symbol.

The block diagrams of the transmitter and receiver are shown on Figures 2.1 and 2.2 respectively. All system users are assumed to have the same diversity order L, and each one of them is assigned a unique address code, represented by a binary vector **a** of length and Hamming weight equal M and L, respectively. The operators $\oplus$ and $\ominus$ represent the modulation and demodulation process, and S_i represents a cyclic shift operation by i position.

At the transmitter, a transmit vector is formed by cyclically shifting the user address code by the symbol value *m*. Each entry in the transmit vector represents a sub-channel. The presence of frequency tones at the set of sub-channels selected to transmit the symbol is indicated by a “1” on the corresponding entries. For unique mapping of each transmit vector to a user-specific symbol, every address code has to be a-periodic; and must not be cyclic shifted versions of one another.

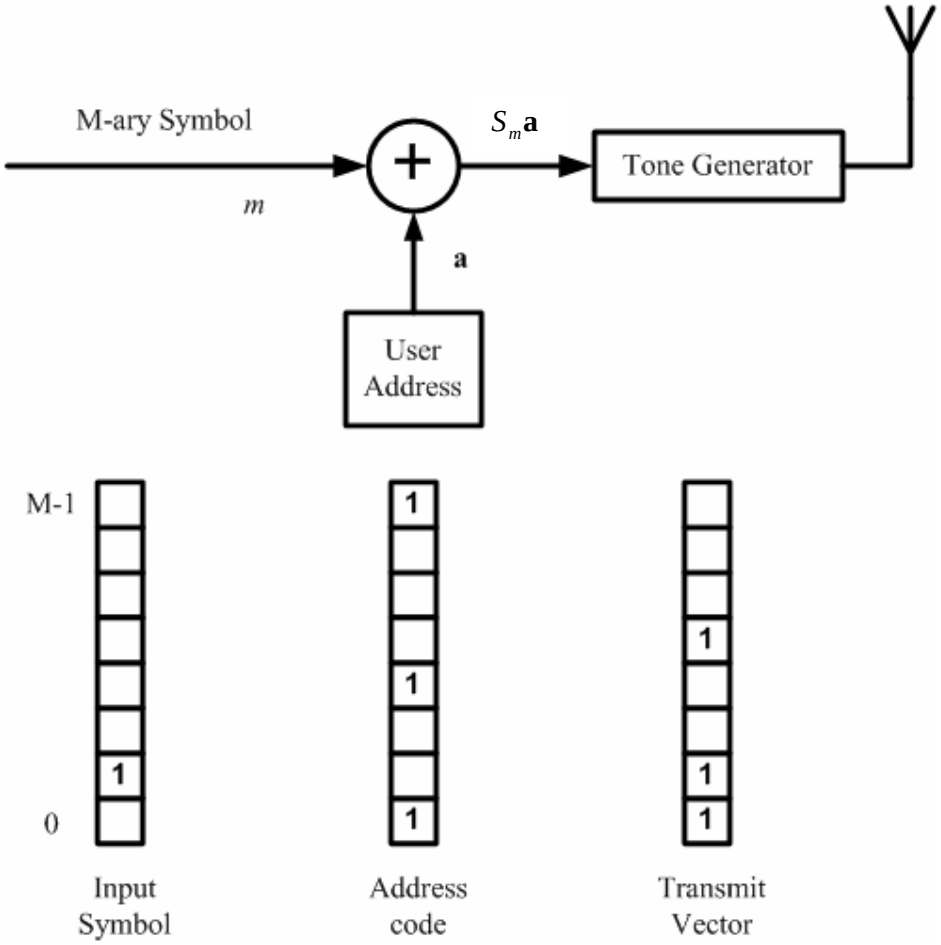

Fig. 2.1 MC-MFSK Transmitter

At the receiver, envelope detector is used on each sub-channel to make a hard decision on the received tone. Note also that individual envelope detector cannot

differentiate between the tones sent amongst the users, and the same output is given even when more than one user transmits on the same sub-channel. A binary received signal vector **v**, is then formed at the spectrum analyzer. The vector **v** represents sub-channels that are transmitted on by at least one user. This vector is then passed to the decoder.

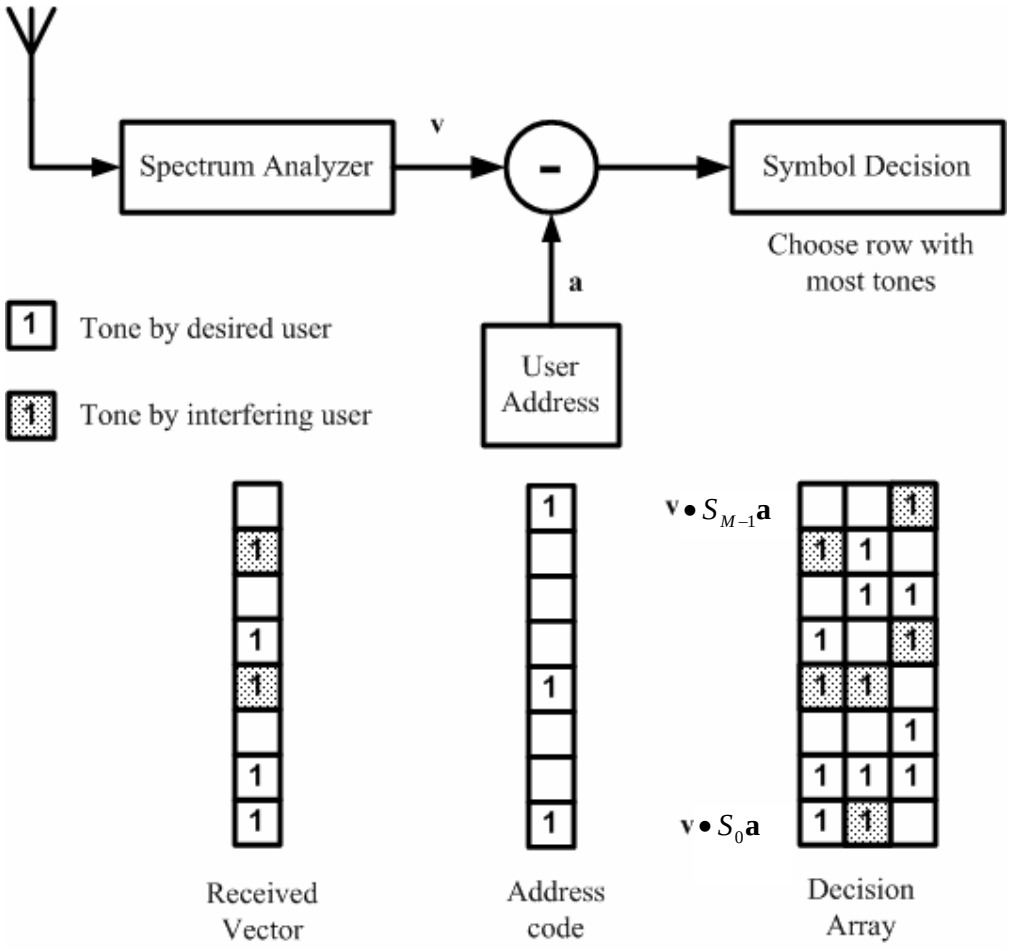

Fig. 2.2 MC-MFSK Receiver

2.2 Decoder

The desired signal is decoded by comparing the correlations of **v** with all possible *M* cyclic-shifted versions of the address vector **a**. The shift associated with the largest

correlation will be decoded as the desired symbol. Mathematically, the decoding rule can be expressed as

$$\hat{m} = \arg\max_{i} \{\mathbf{v} \cdot S_i \mathbf{a}\}, \tag{2.1}$$

where $\hat{m}$ denotes the decoded symbol, and $\cdot$ denotes the dot product operator. In the case where 2 or more shifts have the maximum correlation value, one of these contending shifts is chosen randomly.

The decoding process can also be seen as the selection of a completely occupied row from the M x L decision array. We show the M x L decision array of the MC-MFSK system in Figure 2.2. Each row corresponds to one of the possible symbols. The number of occupied entries in a row reflects the correlation of that symbol.

For a non-fading AWGN channel with high SNR, we assume that each envelop detector makes its decision based on the received tone without error. Hence, the desired symbol always has a complete row filled by its L transmitted tones, while interference from other users and self-interference will scatter and occupy entries in other rows. Decoding error occurs when the interfering tones fill up the row of any erroneous symbol, and the erroneous symbol is selected in the random choice.

2.3 System Capacity and Normalized Throughput

We consider system capacity as the amount of useful information that can be transmitted through the system of symbol error rate, P_e. The diversity order L and modulation level M have significant effect on the error performance of the MC-MFSK system, and hence on the system capacity and throughput. Thus we formulate the

system capacity and normalized throughput for the MC-MFSK system to show the relationship with the system parameters. The MC-MFSK system capacity *C* is similar to the capacity of the multiple-access FH-MFSK system, which is given in [17] as

$$C = P_e \ln(P_e) + (1 - P_e)\ln(1 - P_e) + \ln M - P_e \ln(M - 1), \tag{2.2}$$

in nats per channel use.

We use normalized system throughput as our performance measure, which is defined as

$$W = \frac{K C}{B T_s}, \tag{2.3}$$

where *K*, *B* and T_s denote respectively, the number of user, system bandwidth and symbol duration. Since the MC-MFSK system has *M* sub-channels and frequency separation of $1/T_s$ is used to preserve the orthogonality of each sub-channel, the bandwidth is therefore equal to $B = M \times \frac{1}{T_s}$. We can then simplify (2.3) into

$$W = \frac{K C}{M}. \tag{2.4}$$

In the next chapter, we will derive the optimal system parameters for MC-MFSK systems that will maximize the throughput. We will consider the maximization of throughput for systems subjected to error probability and user number constraints. We also derive the optimal diversity which maximizes the user capacity of MC-MFSK systems with error probability constraint.

Chapter 3

Optimal Diversity Order of Multiple Access Multi-Carrier MFSK Systems

3.1 Introduction

In MC-MFSK systems, the number of frequency-carriers used per symbol transmission is termed the frequency diversity order L. For a given total frequency bandwidth, the diversity order is directly related to the amount of multiple-access interference (MAI) experienced by all users. Hence a trade-off exists between the diversity gain and MAI. Another parameter of interest is the modulation level M. Similar to conventional MFSK systems, the value of M refers to the alphabet size, and also the number of orthogonal sub-channels. We use these two parameters to optimize the MC-MFSK system performance.

Previous analyses [1-3] have evaluated the analytical error probability for MC-MFSK systems in Rayleigh and Rician channels. Computational results show that there exists an optimal diversity order. However, an analytical evaluation of this optimal diversity order has not been made, plausibly due to the complexity of the evaluations.

The objective of this chapter is to work out an analytical solution for the optimal diversity order that maximizes throughput and minimizes error probability. We approach the problem by re-evaluating the system for a non-fading AWGN channel with high SNR, focusing only on the diversity gain and MAI trade-off. A simpler

error rate expression is derived in this case, and we use this expression to find the optimal diversity order. This solution is later verified to approximate the true optimal diversity order, for reasonable SNR under fading channel. We also attempt to optimize the system under various conditions such as an error probability constraint and a fixed number of users.

3.2 Derivation of Symbol Error Rate and Optimization of Diversity Order

3.2.1 Derivation of Symbol Error Rate

We derive an upper bound for the symbol error rate (SER) of MC-MFSK systems based on the following assumptions:

a) Systems in a non-fading, AWGN channel with high SNR
b) All users have a common diversity order and modulation level
c) All users' address codes are distinct and consist of random binary codes

We will show that this channel model can be used to approximate fading channels with high SNR in Section 3.3.

On MC-MFSK modulation, each of the K simultaneous users transmits on L out of M sub-channels. By assuming that users' address codes are random and treating self-interference as equivalent to interference from another external user, the probability of insertion of a tone in an erroneous row is given by

$$P_I = 1 - \left(1 - \frac{L}{M}\right)^K . \tag{3.1}$$

In practice, L/M <<1, and K >>1, hence we approximate P_I as

$$P_I = 1 - \exp(-\frac{LK}{M}) . \tag{3.2}$$

Let P_{filled} denotes the probability that an erroneous row is completely filled. By assuming that the insertion of each entry is mutually independent, an upper-bound for P_{filled} can be formulated as a product of P_I's from L entries,

$$P_{filled} \le \left[1 - \exp\left(-\frac{LK}{M} \right) \right]^L . \tag{3.3}$$

A union bound for the symbol error rate (SER) P_e can then be formulated as [18],

$$P_e \le \frac{1}{2}(M-1)\left[1 - \exp\left(-\frac{LK}{M} \right) \right]^L , \tag{3.4}$$

where the factor ½ accounts for the random choice between the correct and the erroneous symbol.

In Figure 3.1, we compare the union bound derived in (3.4) with the simulation results of MC-MFSK systems in non-fading channel with high SNR. It shows that (3.4) gives a close upper bound to the SER of MC-MFSK systems. For the rest of the chapter, we will consider the SER to be at its worst level. Therefore, we mathematically treat P_e as equal to its upper bound in (3.4).

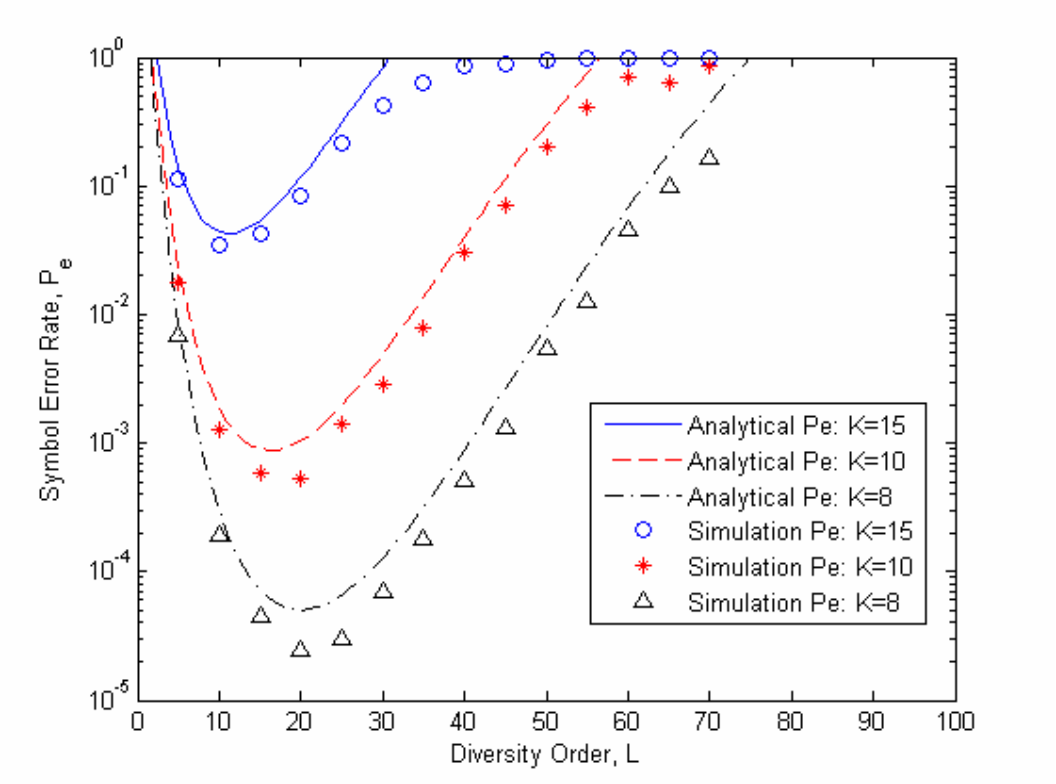

Fig. 3.1 P_e versus L for Analytical and Simulation P_e in non-fading AWGN channel with high SNR channel at $M = 256$

3.2.2 Optimization of Diversity Order

Our objective is to find the optimal diversity order L of MC-MFSK system, which maximizes the normalized system throughput W. From (2.2) and (2.4), we observe that system throughput varies inversely with respect to P_e, for practical region of P_e, i.e. $P_e \le \frac{M-1}{M}$. Hence the optimal L that maximizes throughput W will also minimizes the SER P_e:

$$\max_L \{W\} = \min_L \{Pe\}.$$

Therefore, we minimize the P_e with respect to L by solving,

$$\frac{\partial P_e}{\partial L} = \frac{1}{2}(M-1)\left[\frac{\frac{LK}{M}\exp\left(-\frac{LK}{M}\right)}{1-\exp\left(-\frac{LK}{M}\right)} + \ln\left(1-\exp\left(-\frac{LK}{M}\right)\right)\right] = 0, \tag{3.5}$$

where $\frac{\partial P_e}{\partial L}$ denotes the first partial derivative of P_e with respect to L. From (3.5), we yield for the first time a useful expression of the optimal diversity order [18],

$$L^* = \frac{M}{K}\ln 2. \tag{3.6}$$

3.3 Numerical Results and Comparison

In this section, we present numerical results to compare the optimal diversity order formula in (3.6) with the numerically searched value. This is to prove the validity of our results for MC-MFSK systems in fading channels.

We numerically search for the optimal diversity order by using the SER upper-bound for MC-MFSK systems in fading channel that is derived by Sinha in [2] as

$$P_e < 1 - \sum_{i=0}^{L} P_d(i)\left[P(i,0) + \frac{1}{2}P(i,1)\right]. \tag{3.7}$$

In (3.7) above, $P_d(i)$ denotes the probability that the desired symbol gives a correlation value i; and $P(n,k)$ denotes the probability that among the M-1 erroneous symbols, k symbols gives the maximum correlation value n. The probability of false alarm, P_F (probability that a tone is detected when there is none), and probability of deletion, P_D (probability that a tone is sent but is not detected) are evaluated in [2 (eqn. 16,17)] for Rayleigh channel, and in [3 (eqn 19,20)] for Rician channel.

Using the expression for P_e in (3.7), we numerically search for the optimal diversity order which results in the minimum error rate. We denote the numerically searched optimal diversity order as L_{opt} and our analytical optimal diversity order as L^*.

We compare the cases of {M=1024, K=20} and {M=512, K=10}, in both Rayleigh and Rician channels. An identical Rice factor, K_S = 10, is assumed for all users in the Rician channel. In all the above cases, L^* = 35 (rounded up to the nearest integer). We plot L_{opt} and L^* with respect to the SNR per bit in Figure 3.2, where the SNR is defined as the energy per bit over average AWGN power. We see that the optimal diversity order L^* given by (3.6) becomes closer to the numerically searched optimal diversity order L_{opt} for larger SNR. We also observe that L^* gives a reasonable prediction of the optimal diversity order for SNR equal and above 40 dB.

For SNR below 40 dB and shown in Figure 3.2, the L_{opt} in Rician channel converges to L^* at a lower SNR than L_{opt} in Rayleigh channel. This is due to the Line-of-sight component in Rician channel that allow a more accurate detection of the tones compared to transmission over Rayleigh channel of the same SNR.

We believe that at high SNR, the MAI becomes dominant and effects of fading become negligible. Thus the optimal L predicted by (3.6), which is derived based on the assumption of interference-limited and non-fading channel becomes more accurate.

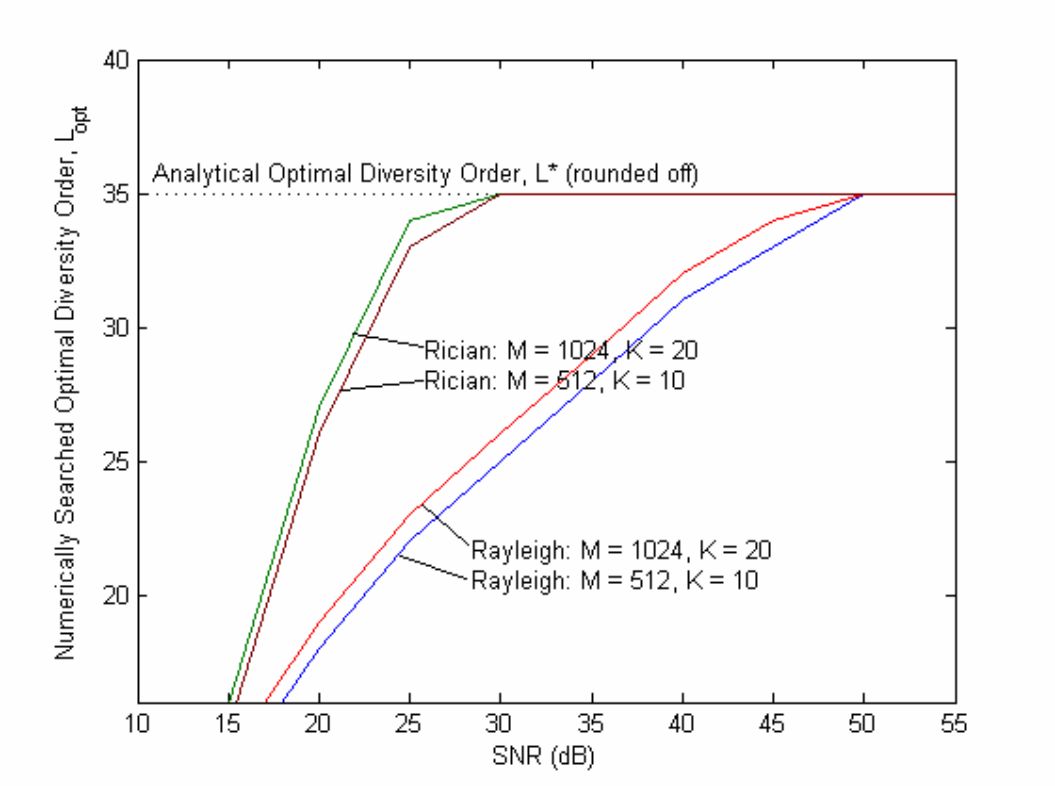

Fig. 3.2 L_{opt} versus SNR for {M=1024, K=20}, {M=512, K=10}. L_{opt} searched using (3.7) for Rayleigh and Rician channels, compared to L* computed from (3.6)

In Figure 3.3, we show the plot of BER versus L for several M, K, and SNR values computed using (3.7). The asterisk on each curve corresponds to the BER performance at optimal diversity order $L = L^*$. We can see that the BER at diversity order, computed from our theoretical result in (3.6), has negligible difference to the minimum value.

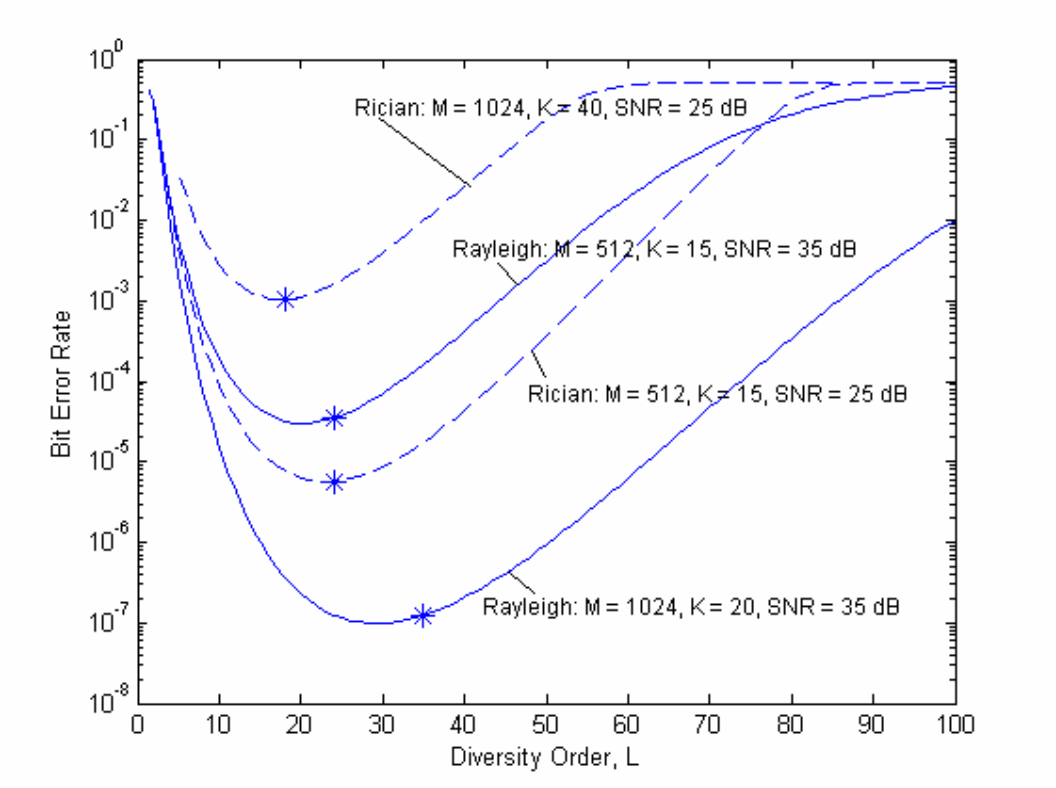

Fig. 3.3 BER versus L for fading channels for various M, K, and SNR, asterisk (*) marks the error performance at optimal diversity order L*

3.4 Optimal Diversity Order for Maximum User Capacity Subject to Symbol Error Probability Constraint

In the previous section, we need to know the number of active users in the system to optimize the system. However as with most multiple-access systems, it is not practical to adjust the diversity order according to changes in the number of users, as users constantly leave or enter the network. In addition, a system is often conditioned to provide every user with a certain level of service quality, in terms of error rate. Therefore, we formulate the following optimization problem: optimal diversity order to maximize the user capacity K_{max} instead, given a SER limit P_0. Mathematically,

$$\max_{L} \{K_{\max}\} \tag{3.8}$$

subject to:

$$P_e \le P_0$$

From (3.4) and (3.6), we find the minimum SER,

$$P_e = \frac{1}{2}(M-1)\left(\frac{1}{2}\right)^{L^*} = \frac{1}{2}(M-1)\left(\frac{1}{2}\right)^{\frac{M\ln 2}{K}}. \tag{3.9}$$

Noting that P_e is monotonic increasing with respect to K, we apply (3.9) to the SER constraint $P_e \le P_0$ and derive the inequality on K as

$$K \le \frac{M\ln 2}{\log_2(M-1) - \log_2(P_0) - 1}. \tag{3.10}$$

The user capacity is reached ($K = K_{\max}$) when P_e is raised to its SER limit, P_0. Therefore the maximum user capacity is derived as

$$K_{\max} = \frac{M\ln 2}{\log_2(M-1) - \log_2(P_0) - 1}. \tag{3.11}$$

Substituting (3.11) into (3.6), an expression of the optimal diversity order L^* for maximum user capacity is derived as

$$L^* = \log_2(M-1) - \log_2(P_0) - 1. \tag{3.12}$$

Both L^* and $K_{\max}$ depend only on the SER limit and M. The optimal diversity order given by (3.12) achieves the maximum user capacity. However this diversity order in (3.12) does not guarantee the minimum error rate when the number of users is below the capacity. Figure 3.4 shows the plot of user capacity against the SER limit.

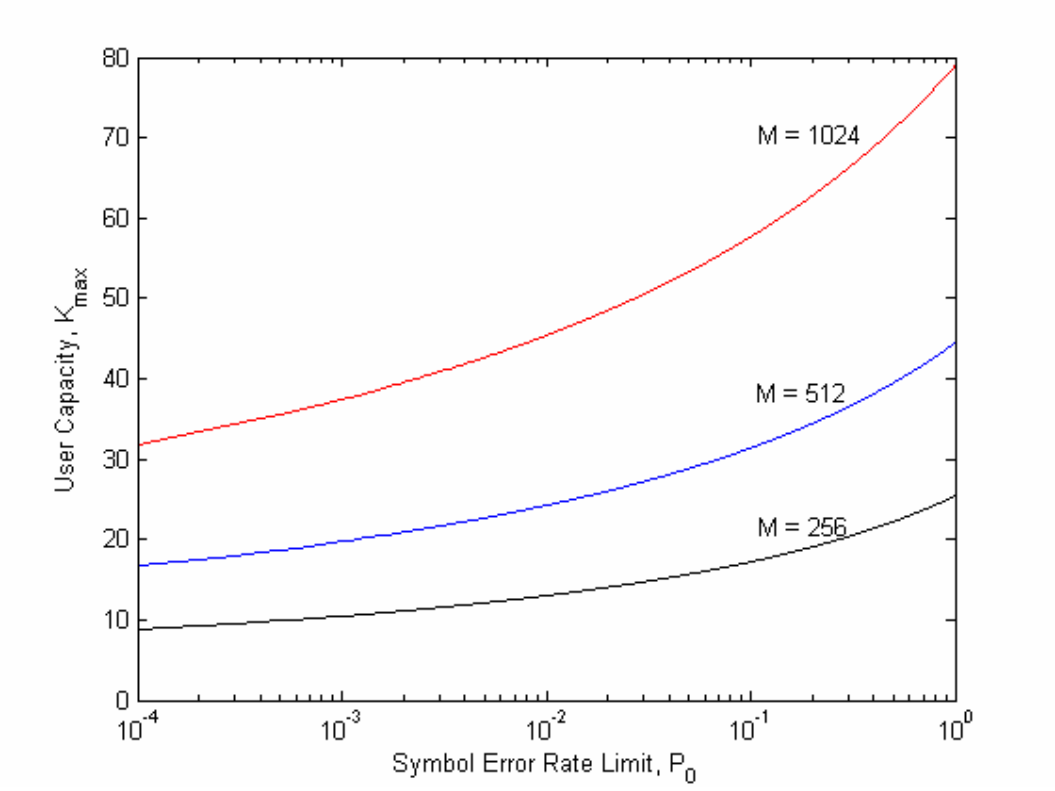

Fig. 3.4 K_{max} versus P_0 at M = 256, 512, 1024

3.5 Throughput Maximization Subject to Symbol Error Probability Constraint and Constant Number of Users

Now we want to maximize the normalized throughput W, given a SER limit P_0 and a fixed number of users K_0. The objective function for this problem can be expressed mathematically as,

$$\max_{L,M}\{W\} \tag{3.13}$$

subject to:

$$K = K_0$$

$$P_e \le P_0$$

We approach this problem by first maximizing W with respect to L only. The solution to this maximization problem is presented in Section 3.2, where the optimal diversity order is given by

$$L^* = \frac{M}{K} \ln 2 . \tag{3.14}$$

Also we derive the minimized symbol error rate P_e (with respect to L) as

$$P_e = \frac{1}{2}(M-1)\left(\frac{1}{2}\right)^{\frac{M \ln 2}{K}} . \tag{3.15}$$

Given (3.14) and (3.15), we want to maximize the throughput W with respect to M next. By numerical computation of W using (2.4), we find that W has a maximum point when M is of value between 3 to 4 at practical P_e values. However this range of M is not useful because it cannot satisfy the P_e constraint for $P_0 \leq 0.1$. According to (3.15), a larger value of M is required to achieve lower SER performance for the system. The computation of (2.4) also shows that beyond the maximum point, W will decrease with M. Therefore, we deduce that the optimal M is the smallest value that satisfies the P_e and K constraints in (3.13). We can numerically solve for this optimal modulation level M^* using

$$\frac{1}{2}(M-1)\left(\frac{1}{2}\right)^{\frac{M \ln 2}{K_0}} \leq P_0 . \tag{3.16}$$

The corresponding optimal L is solved by substituting the optimal M into equation (3.14).

When maximization is performed with respect to a single constraint: $P_e \leq P_0$, there will be no numerical solution to the optimization problem. From (3.15), the number of users K is a factor of M instead and is derived as

$$K = \frac{M \ln 2}{\log_2(M-1) - \log_2(P_e) - 1}. \tag{3.17}$$

Numerical computation of the throughput with K given by (3.17) then shows that normalized throughput W increases monotonically with the modulation level M. For the maximization of throughput W with only SER constraint, this relationship between W and M is not intuitional. The relationship also provides a useful consideration in the design of MC-MFSK systems as follows. Since the bandwidth is directly proportional to M, the system will become more efficient, transmitting more information per Hertz, when operating at a larger bandwidth.

3.6 Conclusion

We have derived the expression for the optimal diversity order in MC-MFSK systems for interference-limited and non-fading channels. At higher SNR where the MAI is the dominating factor, our analytical results can be used to approximate the optimal diversity order L^* for fading channels. Results show that BER performance of systems using L^*, is very close to the simulation results.

In addition, instead of an optimal diversity order for minimizing P_e given the number of users present, we also present solution for an optimization problem of maximizing the user capacity given an error probability constraint.

Chapter 4

Diversity Control in Multiple Access Multi-Carrier MFSK Systems

4.1 Introduction

In this chapter, we study a MC-MFSK system where the base controller does not exist or has no control on the diversity order in each transmitter. Unlike previous works [1,2] where the diversity orders of all transmitters are required to be equal, here the control of all diversity orders is distributed to the individual user.

Note that the diversity order adopted by a user affects the amount of multiple access interference (MAI) experienced by all users. A competing situation thus arises, because each user has the capability to increase its diversity order that will better its performance but increase the level of system-wide interference. There are three issues that we are trying to uncover here:

a) Does a steady state solution for the diversity orders exist?

b) What is this steady state solution if it exists?

c) Is this steady state solution truly “optimal” for the system?

So far, no study has been carried out to address these issues.

Given an initial state where all transmitters begin with arbitrary diversity orders, the system will optimize itself to a set of diversity orders if a steady state exists. Throughout this chapter, we call the steady state solution for the diversity order of

such systems as the optimal diversity order. We evaluate the optimal or steady state diversity orders for the following 2 scenarios:

1) Non-cooperative system users, where the objective of each user is to maximize its own throughput by adjusting its diversity order. The user has no regard on the effect of its action on other users.
2) Cooperative system users, where the objective of each user is to maximize the overall system throughput by adjusting its diversity order. All users cooperate and are assumed to know the performance level of every user.

We will refer to these two scenarios respectively as Case 1 and Case 2 throughout this chapter.

The MC-MFSK system model is as described in Chapter 2. The only difference in this chapter is that each user has its own diversity order. We let L_i denotes the diversity order of user i, and M denotes the modulation level. This time each user is assigned a unique address code, represented by binary vector, $\mathbf{a}_i$ of length equals M and Hamming weight equals L_i.

4.2 Symbol Error Probability, System Capacity and Throughput

In previous works, the authors have analyzed the performance of MC-MFSK systems in the Rayleigh [1,2] and Rician channel [3]. These works lead to complex analytical results, which provide little or no insight on how the diversity order and MAI affect the system performance.

Similar to the evaluation of MC-MFSK system performance in Chapter 3, we derive an upper bound for the symbol error rate (SER) of the distributed diversity control MC-MFSK systems based on the following assumptions:

a) System in a non-fading, AWGN channel with high SNR
b) All users have the same modulation level M
c) All users' address codes are distinct and consisting of random binary codes

The only difference from the previous assumption is that all users do not necessarily have equal diversity order. It is shown in Chapter 3 that this channel model can be used to approximate fading channels with high SNR.

The decoding process for user i can be seen as a particular selection of L_i elements from **v**, to form a row in the M x L_i decision matrix in Figure 2.2. The desired symbol will always have its row completely filled by its transmitted tones, while interference from other users and self-interference will occupy entries in other rows.

The jth user transmits on L_j out of M sub-channels. Considering that the address codes are randomly formed and approximating self-interference as interference by an external user of the same diversity, the probability of insertion of a tone in an erroneous row is given by

$$P_I = 1 - \prod_{j=1}^{K} \left(1 - \frac{L_j}{M} \right) \tag{4.1}$$

where K is the number of active users in the system.

Let $P_{f,i}$ denotes the probability that an erroneous row is completely filled for the *i*th user. We can derive its upper-bound by assuming that the insertion probability for each entry is independent.

$$P_{f,i} \le \left[1 - \prod_{j=1}^{K}\left(1 - \frac{L_j}{M}\right)\right]^{L_i} \tag{4.2}$$

And by union bound, the symbol error probability for the *i*th user is formulated as,

$$P_{e,i} \le \frac{1}{2}(M-1)\left[1 - \prod_{j=1}^{K}\left(1 - \frac{L_j}{M}\right)\right]^{L_i} \tag{4.3}$$

where the ½ accounts for the random choice between the correct and the erroneous symbol.

We now formulate the system capacity and the normalized throughput for MC-MFSK systems. The *i*th user's capacity C_i for an MC-MFSK system is similar to the capacity for the multiple-access Frequency-Hopping MFSK system. This capacity is given in [17] as

$$C_i = P_{e,i}\log(P_{e,i}) + (1-P_{e,i})\log(1-P_{e,i}) + \log M - P_{e,i}\log(M-1). \tag{4.4}$$

Note that for practical range of $P_{e,i}$ ($P_{e,i} < 0.1$), the capacity decreases monotonically with $P_{e,i}$. Hence maximization of the user capacity is equivalent to minimizing its error probability.

We define the normalized throughput W_i for the *i*th user as

$$W_i = \frac{C_i}{BT_s}, \tag{4.5}$$

where B and T_s denote respectively the system bandwidth and symbol duration. Since the MC-MFSK system has M sub-channels and frequency separation of $1/T_s$ is used to preserve the orthogonality of each sub-channel, the bandwidth therefore equals to $B = M \times \frac{1}{T_s}$. We can then simplify the individual throughput in (4.5) to

$$W_i = \frac{C_i}{M}, \quad \forall i = 1, \ldots, K. \tag{4.6}$$

The total system throughput W, is the sum of all K individual throughputs and given by

$$W = \sum_{i=1}^{K} W_i = \frac{\sum_{i=1}^{K} C_i}{M}. \tag{4.7}$$

Both throughputs in (4.6) and (4.7) are respectively the performance measures of Case 1 and 2 in this system.

4.3 Optimal Diversity Order for Multi-Carrier MFSK System

4.3.1 Optimal Diversity Order for Maximizing Individual Throughput

We evaluate the optimal solution for Case 1, where all users adapt only to maximize its individual throughput. Since M is constant, the maximization of individual throughput is equivalent to the minimization of error rate. Hence the objective function is

$$\max_{L_i}\{W_i\} = \min_{L_i}\{P_{e,i}\}, \quad \forall i = 1,\ldots,K\,. \tag{4.8}$$

Denoting the optimal diversity solution as vector $\boldsymbol{L}^* = [L_1^*,\ldots, L_K^*]$, where L_i^* is the optimal diversity order for the ith user, we can evaluate $\boldsymbol{L}^*$ by letting

$$\frac{\partial P_{e,i}}{\partial L_i} = 0 \quad \forall i = 1,\ldots,K\,. \tag{4.9}$$

We approximate (4.9) by using Taylor series expansion and derive

$$\prod_{j=1, j\neq i}^{K} x_j - \prod_{j=1}^{K} x_j + \left(1 - \prod_{j=1}^{K} x_j\right)\left[-\prod_{j=1}^{K} x_j - \frac{1}{2}\left(\prod_{j=1}^{K} x_j\right)^2 - \frac{1}{3}\left(\prod_{j=1}^{K} x_j\right)^3 - \ldots\right] = 0, \quad \forall i, j = 1,\ldots,K \tag{4.10}$$

where $x_j = \left(1 - \frac{L_j}{M}\right)$. By ignoring the third and higher powers of term $\left(\prod_{j=1}^{K} x_j\right)$ in (4.10), we resolve the expression to

$$x_i = -\frac{2}{\prod_{j=1}^{K} x_j - 4}, \quad \forall i, j = 1,\ldots,K\,. \tag{4.11}$$

Since the expressions are symmetric for all K users, we deduce that all L_i^* are equal in the solution for (4.8). Therefore letting $L_i^* = L^*$ for all i and multiplying the equations in (11), a solution for (4.8) can be found by solving the equation (4.12) below [19].

$$\left(1 - \frac{L^*}{M}\right)^{K+1} - 4\left(1 - \frac{L^*}{M}\right) + 2 = 0, \quad L^* \in [1,..., M] \tag{4.12}$$

Hence we prove that a solution exists for the optimized diversity order in Case 1. The users' diversity orders will always converge to this solution at steady state.

4.3.2 Optimal Diversity Order for Maximizing Total System Throughput

We now evaluate the optimal solution for Case 2, where all users will cooperate for the common goal of maximizing the normalized system throughput. Since the system throughput is defined in (4.6) as the sum of individual throughput and M is constant, the maximization of system throughput is equivalent to the maximization of the sum of individual capacities C_i. The objective function can be written as,

$$\max_{L_i}\{W\} = \max_{L_i}\left\{\sum_{j=1}^{K} C_j\right\}, \quad \forall i = 1,\ldots,K \tag{4.13}$$

Hence the necessary condition for the solution $\boldsymbol{L}^*$ is

$$\frac{\partial \sum_{j=1}^{K} C_j}{\partial L_i} = 0 \quad \forall i = 1,\ldots,K \tag{4.14}$$

where

$$\frac{\partial \sum_{j=1}^{K} C_j}{\partial L_i} = \frac{1}{2}(M-1)\left[\ln(P_{e,i}) - \ln(1-P_{e,i}) - \ln(M-1)\right]\left[1-\prod_{j=1}^{K}\left(1-\frac{L_j}{M}\right)\right]^{L_i}$$
$$\times\left\{\ln\left[1-\prod_{j=1}^{K}\left(1-\frac{L_j}{M}\right)\right] + \frac{\frac{L_i}{M}\prod_{j=1,\, j\neq i}^{K}\left(1-\frac{L_j}{M}\right)}{1-\prod_{j=1}^{K}\left(1-\frac{L_j}{M}\right)}\right\}$$
$$+\sum_{r=1, r\neq i}^{K}\left\{\frac{1}{2}(M-1)\left[\ln(P_{e,i}) - \ln(1-P_{e,i}) - \ln(M-1)\right]\left[1-\prod_{j=1}^{K}\left(1-\frac{L_j}{M}\right)\right]^{L_r}\left[\frac{\frac{L_r}{M}\prod_{j=1,\, j\neq i}^{K}\left(1-\frac{L_j}{M}\right)}{1-\prod_{j=1}^{K}\left(1-\frac{L_j}{M}\right)}\right]\right\}. \quad (4.15)$$

Again, since the expressions for $\frac{\partial \sum_{j=1}^{K} C_j}{\partial L_i}$ are symmetric for all K users, we deduce that all L_i* are equal in the solution for (4.13). By letting L_i* = L* for all i and summing the equations in (4.14), the optimal L* is found by solving equation (4.16),

$$\frac{KL^*}{M}\left(1-\frac{L^*}{M}\right)^{K-1} + \left[1-\left(1-\frac{L^*}{M}\right)^{K}\right]\ln\left[1-\left(1-\frac{L^*}{M}\right)^{K}\right] = 0, \quad L^* \in [1,...,M]. \quad (4.16)$$

Similarly for Case 2, we prove that a solution exists for the optimized diversity order [19]. The users' diversity orders will always converge to this steady state solution. Note that the optimal diversity order L* obtain in (4.16) is different from the solution in (4.12), though for both cases all L_i* are equal. Their differences will be discussed in Section 4.5.

4.4 Adaptation of Diversity Order

In simulation we use the following iterative steps for the system users to adapt their diversity order. In each iteration, all users take turn to update their diversity order. We assume that all users are constantly informed of their objective measures. For Case 1, the objective measure is the user's own throughput W_i. For Case 2, the objective measure is the total system throughput $\sum_i W_i$. We denote $L_i(k)$ as the diversity order of user i at the k-th iteration. The adaptation processes involved are,

Step 1: Set $L_i(0) = c_i$, $i = 1,\ldots,K$, where c_i is a arbitrary value, $c_i \in [1,...,M-1]$.

Set iterative index, $k = 0$.

Step 2: Update iteration index $k = k+1$.

For user $i = 1$ to K,

Search $L_i(k)$ that maximize the objective measure.

Replace $L_i(k\text{-}1)$ with $L_i(k)$ for user i.

Step 3: Repeat Step 2 until all $L_i(k)$ converge to a steady state value.

The above iteration is repeated until the system reaches a steady state, where there is no further change in diversity order for all users. Note that the diversity order of all system users always converge to their steady state solution regardless of the order in which the users' diversity orders are updated, or how frequent is their update.

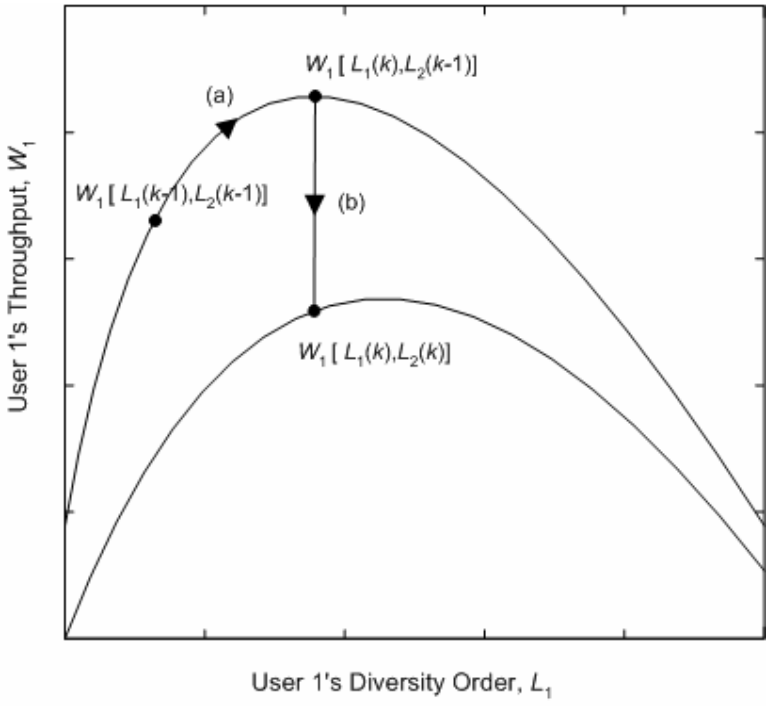

Fig. 4.1 Adaptation of Diversity Order for User 1 (figure not to scale)

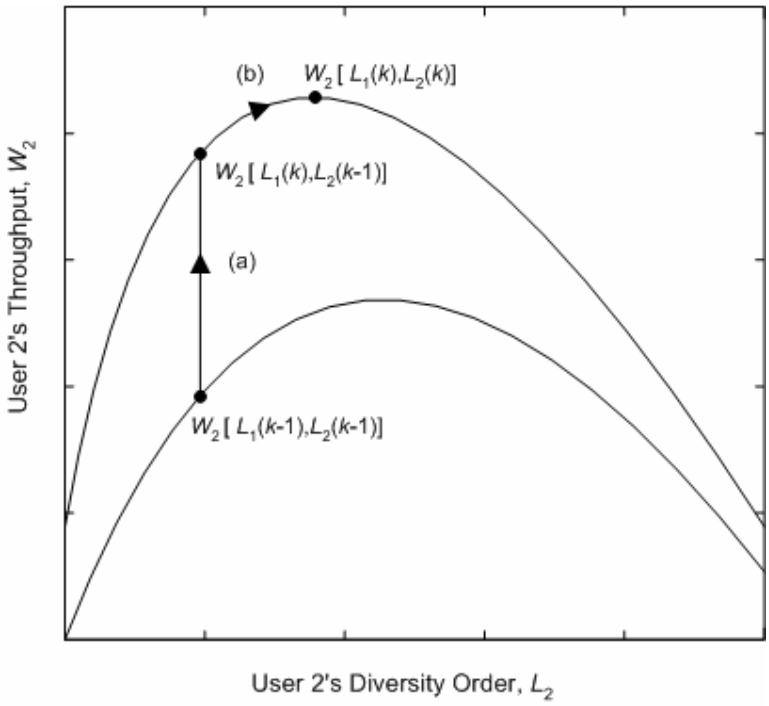

Fig. 4.2 Adaptation of Diversity Order for User 2 (figure not to scale)

Without loss of generality, we illustrate the above iterative steps for a 2-user case. We denote the diversity order of user 1 and 2 at the kth iteration as $L_1(k)$ and $L_2(k)$ respectively. At the start of the kth iteration, user 1 first updates its diversity from $L_1(k\text{-}1)$ to $L_1(k)$ (shown by (a) on Figure 4.1). $L_1(k)$ is the diversity order maximizing user 1's objective measure. This change in user 1's diversity order consequently affects user 2's objective measure (shown by (a) in Figure 4.2).

Next, user 2 updates its diversity order from $L_2(k\text{-}1)$ to $L_2(k)$ (shown by (b) in Figure 4.2). Similarly, $L_2(k)$ is the diversity order maximizing user 2's objective measure at that iteration. The consequential effect on user 1's objective measure is that the maximum point may shift to a different value (shown by (b) in Figure 4.1).

The iteration is repeated for user 1 and 2 until there is no further change in their diversity orders. The diversity orders of both users always converge to the steady solution (4.12) or (4.16) given in Section 4.3.

We carry out simulations for systems with various number of users and arbitrary initial diversity orders. Our results show that their diversity orders indeed converge to the steady state solution (4.12) or (4.16) in Section 4.3.

4.5 Explanation Using Game Theory

Since the system consists of users with conflicting interests, the above results can be explained using the concept of game theory. In game theory, Case 1 and Case 2 of the

diversity control problem are modeled as a non-cooperative game and a cooperative game respectively. We will now summarize two key concepts in game theory:

a) Nash Equilibrium
b) Pareto Efficiency

In the above context, the Nash Equilibrium is defined as a set of diversity orders such that no user can improve its objective measure by unilaterally changing its diversity order. The next concept is the Pareto efficiency. A Pareto efficient point is defined as a set diversity orders where there exist no other set, which at least one user has a better objective measure while the rest remain the same. In other words, a Pareto efficient point is a set of diversity orders where it is impossible to improve the performance of any one user without sacrificing performance of other users. For more detailed explanation of game theoretic concepts for communication systems, readers can refer to works by MacKenzie & Wicker in [20].

For Case 1, all users are at the maximum of their individual throughput at the steady state. None of the system users can increase its throughput unilaterally. Therefore the optimal solution given by (4.12) also represents a Nash Equilibrium point. However it is not a Pareto Efficient point. We can prove this by reducing the diversity order of all users by a small equal amount, and everyone will achieve a higher throughput.

For Case 2, the users achieve the common goal of maximizing the system throughput at steady state. Since the system throughput is the equal-weighted sum of all the individual throughputs, the solution for this case is a set of diversity orders, which no other set can improve the throughput of any user without increasing error probability

of another user. Therefore the solution given by (4.16) is Pareto efficient. We want to point out that the Pareto efficient solution is also the ideal operating point for MC-MFSK systems.

An example of the Nash Equilibrium and Pareto efficient point of a two user system is shown in Figure 4.3 below. Note that L = 118 and L = 40 are the solution to (4.12) and (4.16) respectively, for K=2, M=256. The figure highlights the effect of user 1's diversity order L_1 on the performance of both users. As L_1 increases, the performance of other user will degrade due to the increase in interference level. Also the increase in L_1 will improve user 1's own performance as long as the performance degradation due to self-interference is smaller than the performance gain. The figure also shows that both users achieve a better performance at the Pareto efficient point than at the Nash Equilibrium point.

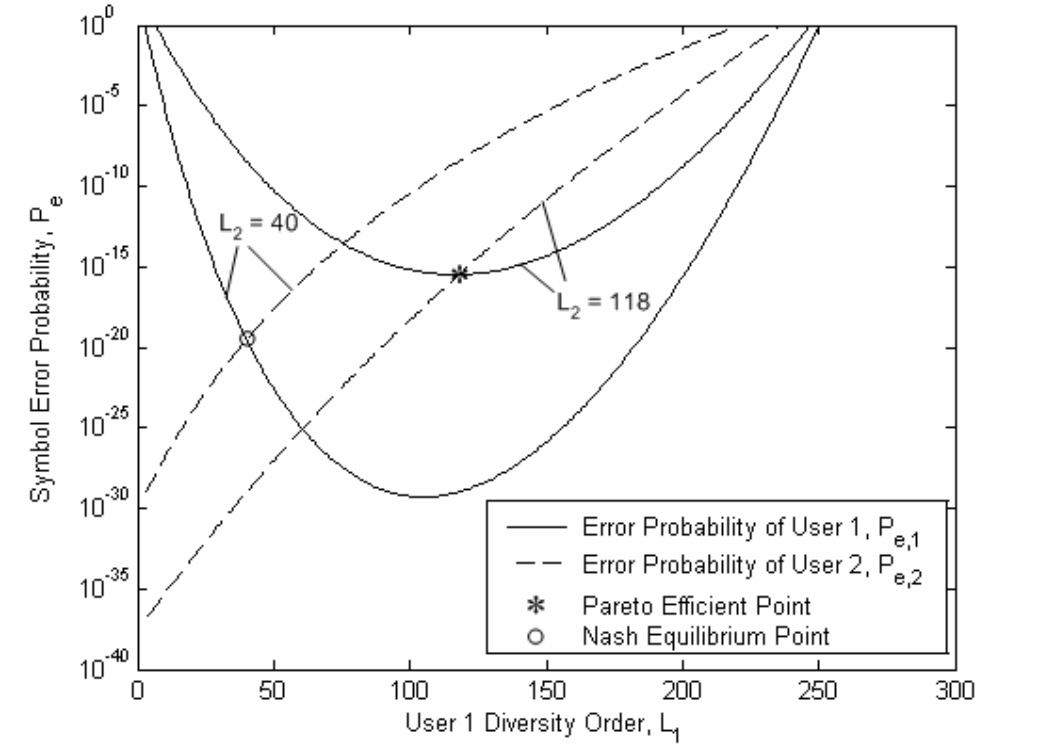

Fig. 4.3 $P_{e,1}$ and $P_{e,2}$ versus L_1 for two user System, M = 256, L_2 = 40 & 118

With the solutions for the Nash Equilibrium and Pareto efficient points, we can also implement policies such as pricing to influence a Pareto improvement to the system for Case 1, such that it can achieve the same level of throughput as Case 2. The users will be imposed with a price that monotonically increases with their diversity order to influence an equilibrium point of lower diversity orders. The price will be a factor in their objective function, and a properly designed pricing can lead the system's equilibrium point to the desired Pareto efficient point. Shah et al. develop such pricing implementation in [21] for power control in CDMA system, which is analogous to our diversity control in MC-MFSK system.

4.6 Conclusion

We have analyzed the characteristic of the Multicarrier MFSK system where control of the diversity orders is distributed to the users. Two scenarios are considered: Case 1 when the users are concern only with its own throughput, Case 2 when the users are concern with the overall system throughput. For each case, we define the appropriate objective function and derive an optimal solution for the diversity orders. Our simulations have verified that the system in both cases always converge to their respective steady operating solutions. We have also explained the results using the concept of game theory. Case 1 is an instance of non-cooperative game and its solution works out the Nash equilibrium point. As for Case 2, its solution works out the Pareto efficient point for the MC-MFSK systems. The Pareto efficient point also represents the desired operating point for Case 1. With these solutions, economic policies such as pricing can be applied in the diversity control of the system. In future

work, pricing policies can be imposed on the users in Case 1 to influence a Pareto efficient equilibrium point.

Chapter 5

Balanced Incomplete Block Design to Improve Performance of Multi-Carrier MFSK Systems

5.1 Introduction

Conventional Multi-carrier Multilevel Frequency Shifted Keying (MC-MFSK) systems [1-3] select the active sub-channels randomly for transmission of each symbol. For the first time in multiple-access MC-MFSK systems, we propose a method of selecting the active sub-channels to improve error performance. We attempt to improve the MC-MFSK system performance by reducing the degree of interference between system users.

In our method, we use a combinatorial construction called Balanced Incomplete Block (BIB) Design. The BIB design is a collection of permutations (as known as blocks) such that any two permutations will have at most λ number of coincidental elements, where λ is a design parameter. The permutations in a BIB design will be distributed among all users, and each permutation will uniquely represent the selection of active sub-channels for each symbol. Hence using our proposed method in the multiple-access MC-MFSK system, symbol transmissions of any two users overlap at most λ number of sub-channels. Therefore the effect of multiple-access interference (MAI) is reduced. For the rest of this chapter, we denote the MC-MFSK system using this method of sub-channels selection based on BIB design as BIB-MC-MFSK system.

Atkins in [6] first uses BIB design to represent the multi-tone signaling of each symbol in multi-tone MFSK modulation. His results show that the BIB design achieves a better error performance and higher bandwidth efficiency than conventional MFSK systems in fading channel, but his works are limited to single-user systems. Our objective is to introduce BIB design in the multiple-access MC-MFSK system to improve performance. By choosing a low value for λ, all sets of active sub-channels have a low degree of coincidence with each other. Hence the users in BIB-MC-MFSK systems will experience a low level of multiple-access interference (MAI). This is unlike conventional MC-MFSK systems where there is no control over the degree of interference.

5.2 Balanced Incomplete Block Design for Multi-Carrier MFSK

A BIB design [7,8] is a collection of b blocks, formed by the arrangement of N distinct elements satisfying the following conditions:

a) each block contains exactly L distinct elements,

b) each element occurs in r blocks, and

c) every pair of distinct elements occurs together in exactly λ blocks.

Any block design that satisfies the above conditions is a BIB design with parameters (N, b, r, L, λ). There are two elementary relationships among these five parameters [7].

$$bL = rN \tag{5.1}$$

$$r(L-1) = \lambda(N-1) \tag{5.2}$$

The first equation is derived by counting the total number of single incidence, while the second equation is derived by counting the number of pairs containing a particular element.

In our method of sub-channels selection, we use each block of the BIB design to represent the multiple sub-channels transmission of each symbol. For example in a BIB design with parameter (N=7, b=7, r=3, L=3, λ=1), the blocks are given by [(0 1 2), (0 3 4),(1 4 5),(2 5 3),(6 3 1),(6 4 2),(6 5 0)]. Each block contains the permutation of the active sub-channels, such as block (0 1 2) means that sub-channel 0, 1 and 2 are selected. These blocks are divided among the users. Within each user, each block is uniquely assigned to a symbol.

We show a block diagram of the BIB-MC-MFSK transmitter in Figure 5.1. The BIB-MC-MFSK system will transmit using the assigned blocks in the same way as the conventional MC-MFSK system using its assigned random code. The details on the transmitting and receiving process can be found in Chapter 2.

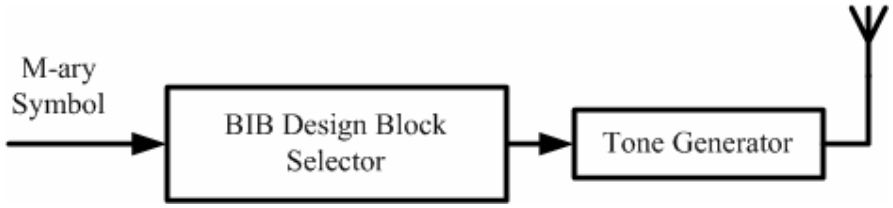

Fig. 5.1 BIB-MC-MFSK Transmitter

Since each of the N elements refers to a distinct sub-channel, the total number of sub-channels in BIB-MC-MFSK systems is N. Note that unlike conventional MC-MFSK systems, the number of sub-channels in BIB-MC-MFSK is independent of the

modulation level M. Also each block will select a permutation consisting of L sub-channels. Therefore, L represents the frequency diversity order in the BIB-MC-MFSK system.

In this analysis, we consider designs where λ=1. Hence, any 2 distinct blocks will coincide in at most 1 element. BIB designs with λ=1 are also known as Steiner Systems. Due to the relationships in (5.1) and (5.2), a BIB design is only dependent on 2 of its parameters. We will express all formulation in terms of L and N, because L determines the type of BIB construction method and the diversity order of the system, while N affects the bandwidth requirement of the system. However, note that BIB designs do not exist for all combinations of N and L.

5.3 Analysis and Derivations

5.3.1 Derivation of User Capacity and Bandwidth Efficiency

For the modulation level M, each user will require M number of blocks. Since the number of blocks in BIB designs is finite and given by b, there is a limit on the number of users which the system can support. We denote this user capacity as $K_{\max}$ and it is given as,

$$K_{\max} = \left\lfloor \frac{b}{M} \right\rfloor = \left\lfloor \frac{N(N-1)}{L(L-1)M} \right\rfloor, \tag{5.3}$$

where $\lfloor \bullet \rfloor$ denotes a floor function.

To preserve the orthogonality of the sub-channels, a frequency separation of $1/T_s$ must be maintained, where T_s is the symbol interval. Since the BIB-MC-MFSK system will require N number of sub-channels, therefore the bandwidth of the system W is given by $W = \frac{N}{T_s}$. Taking $T_s = T_b \log_2 M$, where T_b denotes the bit interval, we derive the bandwidth efficiency η [22] as

$$\eta = \frac{1/T_b}{W} = \frac{\log_2 M}{N}. \tag{5.4}$$

In contrast, for a conventional MC-MFSK system described in Chapter 2, its number of sub-channels is fixed as M. Hence bandwidth efficiency η of a conventional MC-MFSK system is given as

$$\eta = \frac{\log_2 M}{M}. \tag{5.5}$$

5.3.2 Derivation of Error Probability

In this section, we analyze the error performance of BIB-MC-MFSK systems that is due solely to its multiple-access interference (MAI). We also assume a non-fading AWGN channel with high SNR as in Chapter 3, and the BIB blocks are randomly assigned among the various users.

As presented in the MC-MFSK system model at Chapter 2, a decoding error will occur when the erroneous symbol has more sub-channels occupied than the desired symbol. When erroneous and the desired symbols have equal number of sub-channels occupied, a random choice is made among the contending symbols. Since perfect

channels are assumed, a decoding error will only occur when an erroneous symbol has all its sub-channels occupied and is selected in the random choice.

Given that in BIB design, each element (sub-channel) occurs in exactly r blocks, and there is at most 1 coincidence. There will be x number of interfering blocks for every erroneous symbol, where x is given by

$$x = L(r-1) = \frac{L(N-L)}{L-1}. \tag{5.6}$$

The probability of each user interfering on a erroneous symbol is then given by $x/b-1$. For K number of users ($K \leq K_{\max}$), and assuming the interference of each user to be independent of one another, the number of interfering users Q can be assumed to have a binomial distribution,

$$P(Q=q) = \begin{cases} \binom{K}{q}\left(\frac{x}{b-1}\right)^{q}\left(1-\frac{x}{b-1}\right)^{K-q}, & q = 1,\ldots,K \\ 0, & \text{otherwise} \end{cases}. \tag{5.7}$$

Considering any erroneous symbol, each interferer will occupy only 1 of the L sub-channels with equal probability. Therefore, the probability that all L sub-channels being filled by Q interferers is given as

$$P_{filled}(Q) = C(L,Q) \times \left(\frac{1}{L}\right)^{Q}, \tag{5.8}$$

where $C(L,Q)$ represents the number of interference patterns satisfying the condition of $P_{filled}(Q)$. We need to derive $C(L,Q)$ as follows.

We group the interference patterns into classes of coincidence count. Each coincidence count is expressed as an L dimension vector $\mathbf{g} = [g_1, g_2, \ldots, g_L]$, where g_i represents the number of interferer occupying the ith sub-channel, therefore $\sum_{i=1}^{L} g_i = Q$. The number of distinct permutations for each coincidence count is given by $\frac{Q!}{\prod_{i=1}^{L} g_i!}$. For interference patterns that occupy all sub-channels, they are grouped under **g** such that

$$g_i \geq 1, \text{for } i = 1, \ldots, L. \tag{5.9}$$

Summing the number of permutations in all **g** that satisfy (5.9), we derive

$$\begin{aligned} C(L,Q) &= \sum_{g_1=1}^{Q-L} \sum_{g_2=1}^{Q-L-G(1)} \cdots \sum_{g_{L-1}=1}^{Q-L-G(L-2)} \frac{Q!}{\prod_{i=1}^{L-1} g_i \times [Q - G(L-1)]!} \\ &= \sum_{i=1}^{L} (-1)^{L+i} \binom{L}{i} i^Q \end{aligned}, \tag{5.10}$$

where $G(a) = \sum_{i=1}^{a} (g_i + 1)$. Therefore, the probability of an erroneous symbol having all its sub-channels filled by interference is,

$$\begin{aligned} P_{filled} &= \sum_{Q=1}^{K} P_{filled}(Q) P(Q) \\ &= \sum_{i=0}^{L} \binom{L}{i} (-1)^{L-1} \left[1 - \frac{x(L-i)}{(b-1)L} \right]^K \end{aligned}. \tag{5.11}$$

An alternative approach to derive P_{filled} which gives same result can be found in [23]. Using union bound, we derive the new expression for the upper bound of the symbol error probability (SER) [24] as

$$P_e \le \frac{1}{2}(M-1)P_{filled} = \frac{1}{2}(M-1)\sum_{i=0}^{L}\binom{L}{i}(-1)^{L-1}\left[1-\frac{L(L-i)}{N+L-1}\right]^K, \qquad (5.12)$$

where the factor ½ accounts for the random choice between the correct and the erroneous symbol. The bit error rate is then given by

$$\text{BER} = \frac{M/2}{M-1}P_e. \qquad (5.13)$$

5.4 Effect and Selection of Various BIB Design Parameters

5.4.1 Optimal Diversity Order for Minimum Error Rate

The performance of BIB-MC-MFSK systems for varying L is evaluated using (5.13) and shown on Figure 5.2. We observe that an increasing L will improve the BER performance. This effect is known as the diversity gain. Since each BIB block can only coincide on at most 1 sub-channel, hence at higher L, the error probability decreases as more sub-channels of the erroneous symbols have to be occupied. This is unlike the case for random code, where increasing L increases the degree of self interference.

However there is trade-off for the diversity gain. As L increases while the number of sub-channels N remains constant, the technique of sub-channels selection based on BIB design will have lesser number of blocks that can still coincide on at most 1 sub-

channel. Thus the user capacity K_{max} will decrease for increase in L. This relationship is shown on (5.3), and on the decreasing K limit of the lines in Figure 5.2. Thus the optimal choice of diversity order L is the largest possible value of L under the constraint $K < K_{max}$.

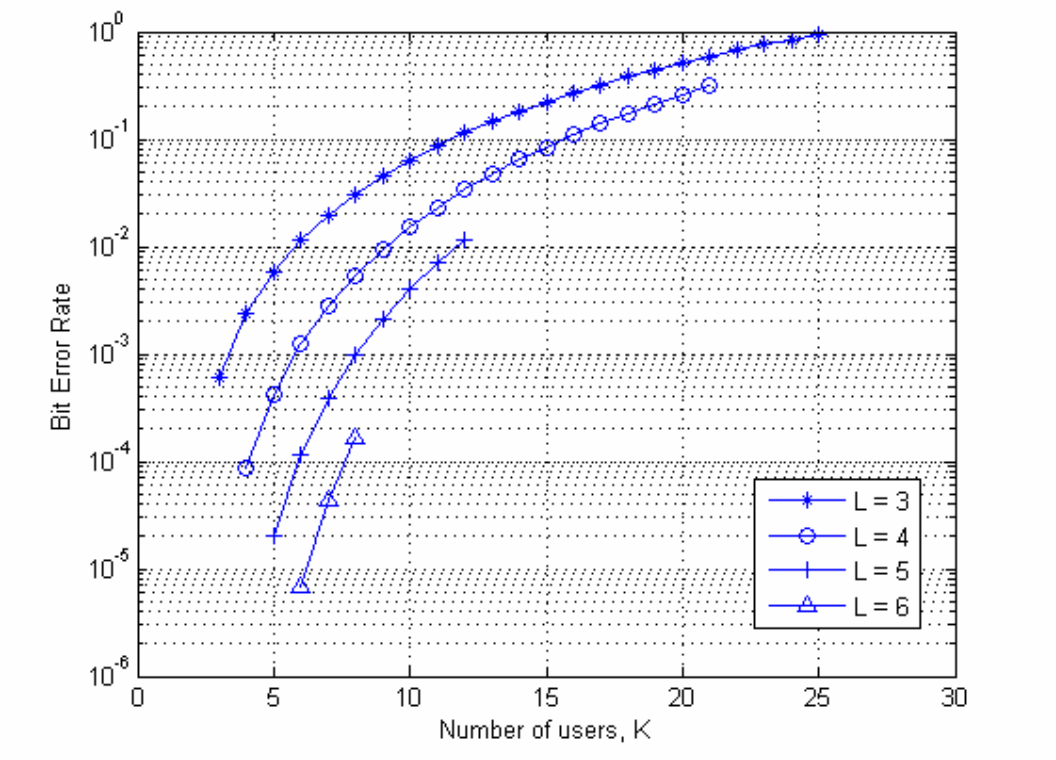

Fig. 5.2 Analytical BER versus number of users K for M=256, N=256 and various L, where the decreasing K limit on the lines are due to lowering user capacity as L increase. BER performance improves with increases in L.

5.4.2 Optimal Modulation Level for Maximum User Capacity at Constant Bandwidth Efficiency

For constant bandwidth efficiency, $\eta = 1/c$ where c is an arbitrary constant, we have

$$N = c \log_2 M \,. \tag{5.14}$$

Applying (5.14) to (5.3), we can re-write $K_{\max}$ as

$$K_{\max} = \left\lfloor \frac{c \log_2 M \times \left(c \log_2 M - 1\right)}{L(L-1)M} \right\rfloor. \tag{5.15}$$

Since the floor function $\lfloor \bullet \rfloor$ is monotonic and L is treated as constant, the maximization of $K_{\max}$ with respect to M is equivalent to maximization of the function,

$$f(M) = \frac{c \log_2 M \times \left(c \log_2 M - 1\right)}{M}. \tag{5.16}$$

We can solve for the optimal modulation level M^*, which maximize $f(M)$, as

$$M^* = \exp\left[\frac{2c + \ln 2 + \sqrt{4c^2 + (\ln 2)^2}}{2c} \right]. \tag{5.17}$$

In practice, $c \geq 1$, therefore the optimal modulation level falls within a narrow range of $7.39 \geq M^* \geq 11.1$, which corresponds to the convention value of M=8 for binary systems. Hence, we can maximize $K_{\max}$ when taking M towards a conventional value of 8.

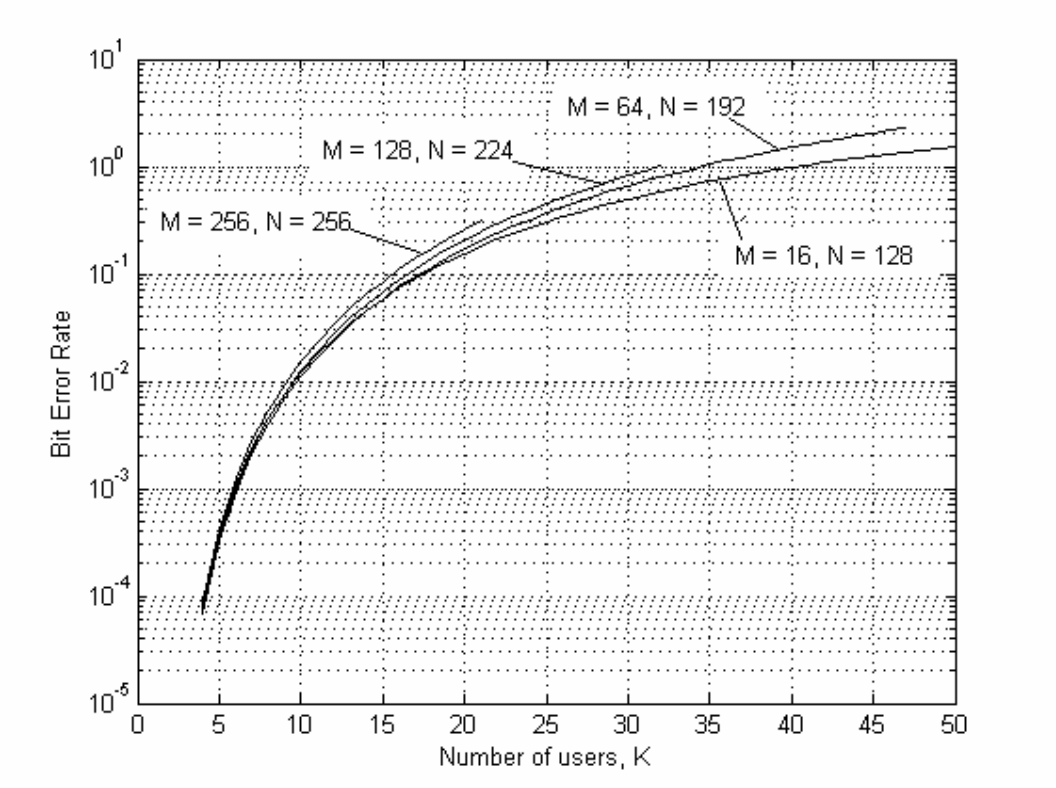

Fig. 5.3 Analytical BER versus number of users K for $\eta = 1/32$, $L = 4$ and various M

In addition, the bit error rate is relatively unchanged for variation in M when η is kept constant. An example of its independence from M for $\eta = 1/32$ is shown on Figure 5.3. Therefore the error performance is not degraded when this optimal M is used.

5.4.3 Selection of BIB Design Parameters for Maximum Error Performance at Constant Bandwidth Efficiency

To select the BIB design parameters which maximize error performance at constant η in BIB-MC-MFSK systems, we must take into consideration the effects of parameters L and M simultaneously. The modulation level M will first be set at the optimal value, but with the purpose of keeping the constraint $K < K_{max}$ satisfied so we can employ the

largest diversity order L. We then look for suitable BIB design parameters by searching through a list of existent design parameters. Using the choice of M value and (5.4), we will select design parameters that allows for a BIB-MC-MFSK system of bandwidth efficiency η reasonable close the required value, and have a large diversity order L.

Note that BIB designs do not exist for all combinations of design parameters N and L, thus there may not exist a pair of design parameters $\{N, L\}$ that results in the required η when M=8. For the same reason, there might also be designs at other values of M that result in the required η and with larger L, and thus better performance. Therefore M^*=8 serves only as a guide for the parameter choice of M. The search for suitable design parameters $\{N, L\}$ must also be done for adjacent values of M in the binary system, such as M=4 and M=16. We will illustrate the selection of suitable design parameters $\{N, L\}$ by an example below.

In this example, we want to first choose suitable parameters of BIB designs for $1/\eta$=32. We use the inverse of bandwidth efficiency $1/\eta$ as a clearer quantity to present and to compare the bandwidth efficiencies. We will search through a list of existent of BIB design parameters $\{N, L\}$ on Table 5.1, and choose designs that have $1/\eta$ reasonably close to 32 for cases of M=4, 8 and 16. Table 5.1 lists examples of existent BIB designs parameters $\{N, L\}$ from [7].

The design parameter pairs that satisfy $1/\eta \approx 32$ are highlighted on the table. Out of these designs we select designs with large diversity order. In this example we will

select BIB designs of parameter set {N=91, L=10, M=8} and {N=121, L=11, M=16}. In the next section, we will apply these two designs in the simulation of BIB-MC-MFSK systems for a performance comparison with conventional MC-MFSK systems.

Table 5.1 Examples of existent BIB designs

BIB Design Parameter		Inverse of Bandwidth Efficiency, $1/\eta$		
L	N	$1/\eta$ when M=4	$1/\eta$ when M=8	$1/\eta$ when M=16
6	31	15.50	10.33	7.75
	126	63.00	42.00	31.50
7	49	24.50	16.33	12.25
	343	171.50	114.33	85.75
8	57	28.50	19.00	14.25
	64	32.00	21.33	16.00
9	73	36.50	24.33	18.25
	81	40.50	27.00	20.25
10	91	45.50	30.33	22.75
	730	365.00	243.33	182.50
11	121	60.50	40.33	30.25
	1331	665.50	443.67	332.75
12	133	66.50	44.33	33.25
	1332	666.00	444.00	333.00

5.5 Performance Comparison with Conventional Multi-Carrier MFSK Systems

We now present simulation results on the BIB-MC-MFSK system in the Rayleigh fading channel, and compare its performance with the conventional MC-MFSK system for a similar η. We assume that the conventional MC-MFSK system constantly adopts the optimal diversity order as presented in Chapter 3. Note that for different number of users *K*, the diversity order for the conventional system will change accordingly, to its optimal value give by the expression $L = \frac{M \ln 2}{K}$. To compare with a conventional MC-MFSK system of modulation level, $N = M = 256$ and hence $1/\eta = 32$; we simulate BIB-MC-MFSK systems of the parameter sets {N=91, L=10, M=8} and {N=121, L=11, M=16}, with $1/\eta$ of 30.3 and 30.25 respectively. The selection of these sets of optimal BIB design parameters is shown at the example on section 5.4.3. Since the systems operate on different modulation level, we compare their error performances by their bit error rate. Under a common bit rate and bit SNR, all the above systems utilize a similar amount of system resources.

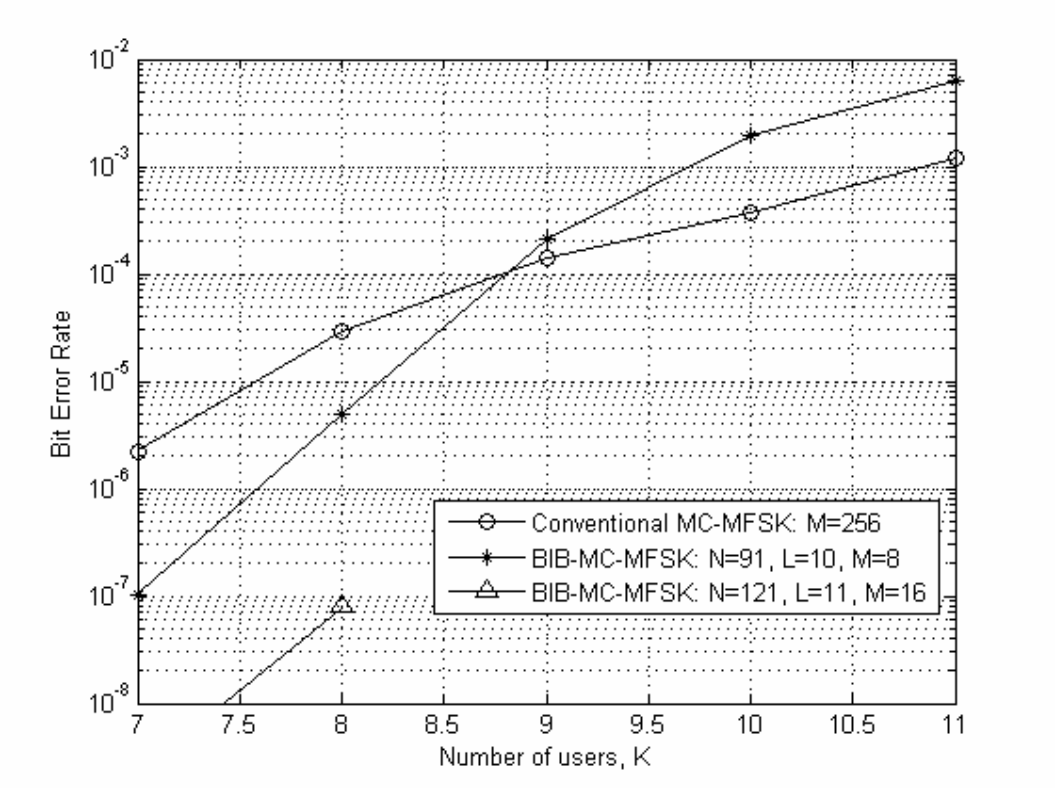

Fig. 5.4 BER versus number of users *K* for BIB-MC-MFSK and conventional MC-MFSK systems in Rayleigh Channel and with Bit SNR = 40 dB

The comparison is shown on Figure 5.4. Based on the performance of BIB-MC-MFSK systems with parameter set {*N*=91, *L*=10, *M*=8}, we observe that there is a crossing point in *K*, where below it, BIB-MC-MFSK systems achieve better BER performance than conventional MC-MFSK systems. The improvement increases as the number of users *K* is lower than the switching point. However, the BIB-MC-MFSK system performs worse for *K* greater than the switching point.

The quantitative variation of this switching point with different parameter set is not uncovered. Hence for any parameter set, the range of *K*, which gives a better performance, is derived only by performance comparison as exemplify in Figure 5.4.

The improvement by BIB-MC-MFSK systems is shown at lower value of K because, at that region, multiple-access-interference alone is unable to cause decoding error. As described in the system model of MC-MFSK systems, an erroneous symbol must have all its L sub-channels occupied for error to occur. Since interference occupies at only one sub-channel per interferer in the BIB-MC-MFSK system, interference occupy at most K out of L sub-channels when the number of users K is less than the diversity order L. For the decoding error to occur, fading effects such as false alarm or deletion will have to occur on specific sub-channels. For example, false alarms occurring on the remaining un-interfered sub-channels, or deletions occurring on the desired symbol's sub-channels. The probability of these occurrences on the specific sub-channels is low, and the probability further reduces when the difference between K and L increases. Thus the error probability will vary with K correspondingly.

Also in Figure 5.4, the BIB-MC-MFSK system with parameter set $\{N=121, L=11, M=16\}$ is shown to achieve a better error performance than the BIB-MC-MFSK system with parameter set $\{N=91, L=10, M=8\}$. This result is because the former system employs a larger diversity order. However, as mentioned in section 5.4.1, the trade-off is that the system has a smaller user capacity of 8 users.

The BIB-MC-MFSK system of both parameter sets achieves better error performance than the conventional MC-MFSK system at region of low K. Therefore we deduce that BIB design is a useful technique for selecting the active sub-channels when the number of users is low.

5.6 Conclusion

In this chapter, we have proposed a method of sub-channels selection based on BIB design to improve the MC-MFSK system performance. This is the first time a deterministic design has been used to select the sub-channels in MC-MFSK systems. The selections of sub-channels will represent each symbol of every user. Using BIB design, any two of these selections will overlap in at most one sub-channel, thus reducing the degree of interference in the system. By analyzing the system model under perfect channel, we have derived expressions for the error rate and user capacity of our BIB-MC-MFSK system. From the analysis of these expressions for the various system parameters, we find the optimal diversity order and optimal modulation level that respectively maximize the error performance and user capacity. Also we introduce a selection method for optimal parameters of BIB design which maximizes error performance for constant bandwidth efficiency. We compare the performance of the BIB-MC-MFSK system with the conventional MC-MFSK system by simulation. Both systems are simulated at their optimal parameters and under a Rayleigh fading channel. Although the BIB-MC-MFSK system perform worse than the conventional MC-MFSK system when number of users is large. We find that the BIB-MC-MFSK system achieves significantly better bit error performance for lower number of users. With appropriate choice of parameters for BIB design in the system, the improvement in performance can be more than ten times.

So far we have studied the MC-MFSK system which do not employ time diversity. In the next chapter, we will extend the system by introducing frequency hopping. We shall evaluate the performance and characteristics of this so-called Frequency-

Hopping Multi-carrier MFSK system. Previous analytical results, such as optimization of diversity order and usage of BIB design, can be applied in this system.

Chapter 6

Extension to Frequency-Hopping Multi-Carrier MFSK Systems

6.1 Introduction

Now we explore an extension of the MC-MFSK system by including a frequency-hopping component. We call the extended system the Frequency-Hopping Multi-Carrier MFSK (FHMC-MFSK) system. Previously in MC-MFSK systems, a set of frequency sub-channels are used simultaneously for transmission over the symbol interval. Now in FHMC-MFSK systems, the transmission occurs over several time hops (or chip interval) and a different set of sub-channels will be used at each time hop.

The FHMC-MFSK system possesses both frequency diversity and time diversity. The frequency diversity is parameterized as the average number of transmitting sub-channels per time hop, and the time diversity is parameterize as the number of time hops per symbol. We use L to denote frequency diversity due to MC-MFSK transmission and use H to denote time diversity due to frequency hopping. Since the FHMC-MFSK system retains inherent frequency diversity as in the MC-MFSK system, it inherits the advantages of the MC-MFSK system such as robust performance against fading effects. The FHMC-MFSK system also has the benefits of near-far immunity and high spectral efficiency. Likewise, the FHMC-MFSK system

can be easily implemented by making use of OFDM based technology, the IFFT/FFT operations eliminate the need for banks of oscillators [1].

The FHMC-MFSK system is first introduced by Timor [15] and then by Mabuchi et al. [16] for use in mobile radio. Like previous works in [2,3], an optimal diversity order is observed in Timor and Mabuchi's results, however, they did not make an analytical evaluation for it. We believe that by applying the same analysis as in Chapter 3 to this FHMC-MFSK system, we can extend the earlier contributions to this new system. Hence, we can advance both the MC-MFSK system and its frequency-hopping variant, the FHMC-MFSK system, as candidates for future high speed communications systems.

In this chapter, we will first describe the FHMC-MFSK system model. We then study the different types of random codes that can be applied to the system and discuss their performance and implementations. Using the approach in Chapter 3, we present a mathematically simpler expression for the error performance of FHMC-MFSK systems than previous works [15,16]. From the expression, we then derive an analytical solution for the optimal frequency diversity. Lastly, a discussion on the effect of various system parameters, such as diversity order and modulation level, is presented.

6.2 Frequency-Hopping Multi-Carrier MFSK System Model

In FHMC-MFSK systems, the channel is divided into its frequency sub-channels and time hops. For each symbol transmission, a tone will be transmitted on a permutation of sub-channels over different time hops. Hence each symbol can be represented by a

binary Frequency-Time (FT) matrix/code as shown in Figure 6.1. Considering that the system utilizes N frequency sub-channels and H time hops per symbol, the matrix will be of size N x H. Note that in FHMC-MFSK systems, the total number of sub-channels N need not be equal to the modulation level M. The FT matrix denotes the signaling pattern of the symbol, where the column and row position of the selected entries (indicated by "X") denote the transmitting sub-channel's index and hop interval respectively. The matrix representation of each symbol must be unique among all users. We assume that all users in FHMC-MFSK systems operate with the same number of time hops H and the same mean number of sub-channels per hop L. Therefore the FT matrices used are all of the same weight with the value $L \cdot H$.

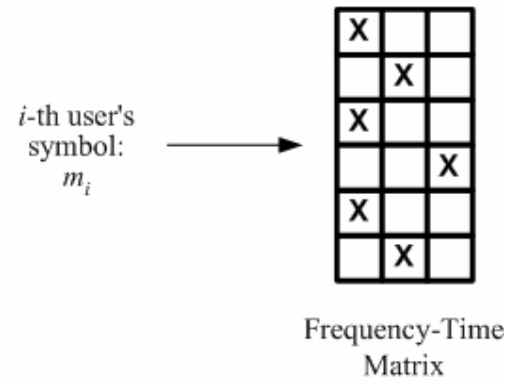

Fig. 6.1 Frequency-Time matrix representation

Note that Goodman's FH-MFSK system [9] and Sinha's MC-MFSK system [1,2], can be considered as special cases of this FHMC-MFSK system where L=1 or H=1 respectively.

At the receiver, envelope detector on each sub-channel will determine if a tone is transmitted. This hard decision is made at every hop interval, and the results will form

a N x H received energy matrix $\boldsymbol{R}$. Under a perfect channel, $\boldsymbol{R}$ is composite (OR sum) of all K frequency-time matrixes of the transmitted symbols, where K represents the number of users.

For a modulation level M, every user will be assigned M number of FT matrixes to represent each of its M symbols. Each user decodes its symbol by correlating its assigned FT matrixes with $\boldsymbol{R}$. This decoding process can be visualized as a selection of $L \cdot H$ entries from $\boldsymbol{R}$, where locations of the $L \cdot H$ entries are based on each assigned FT matrix. Each selection is then arranged as a row in the decision matrix $\boldsymbol{D}$. Hence there will be M number of rows in $\boldsymbol{D}$, and the size of the decision matrix $\boldsymbol{D}$ for each user will be M x $L \cdot H$. Each row in $\boldsymbol{D}$ corresponds to a symbol, and the number of occupied entries on any row reflects the correlation of that symbol. The decoder will select the symbol with the greatest correlation, and in cases of more than one symbol having the maximum correlation, a random choice is made among the contending symbols. An example of the decoding process is shown in Figure 6.2.

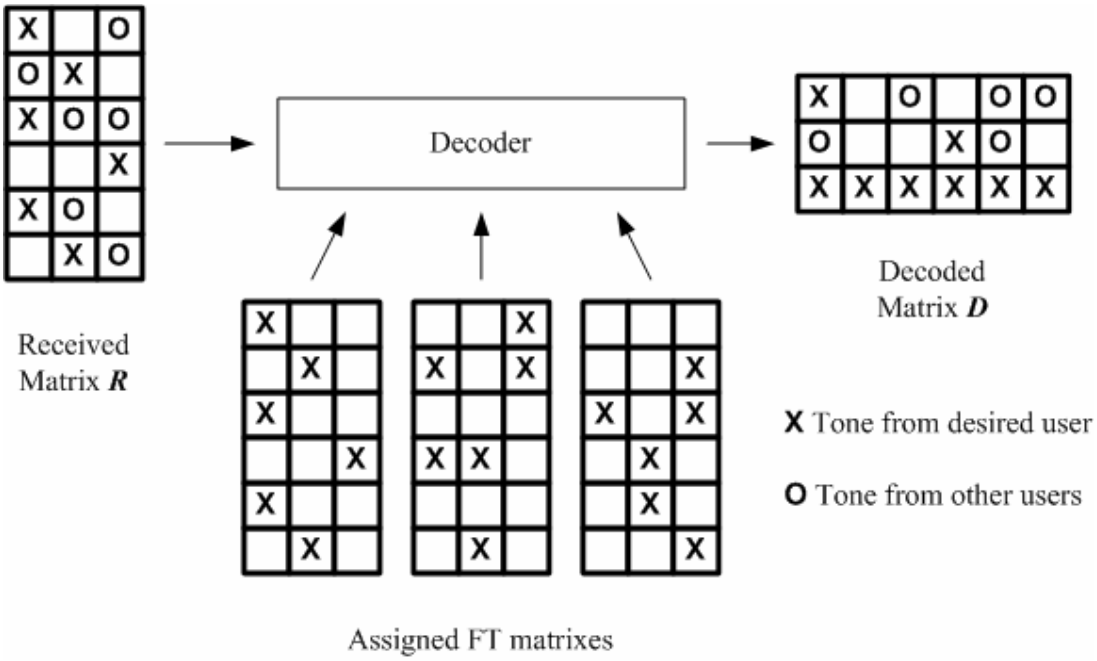

Fig. 6.2 FHMC-MFSK system decoding process

For a perfect channel, the correct symbol always has a complete row filled by its $L \cdot H$ transmitted tones, while interference (from other users and self-interference) will scatter and occupy entries in other rows randomly. A decoder error will occur when an erroneous row either 1) has more occupied entries than the desired row, or 2) has the same number of entries as the desired row and is chosen in the random choice. Due to the intrinsic multiple access interference (MAI) in the system, such error can occur, even in the absence of fading and AWGN.

6.3 Types of Random Frequency-Time Code and Comparison

As we extend the system to include frequency-hopping, there arises various methods which the FHMC-MFSK encoder can be implemented. Therefore, different forms of random FT codes/matrixes can be generated. These codes can be distinguished by the presence of two properties:

a) The number of tones at each hop is constant and equal to L.

b) Codes for the same user are cyclic-shifted version of each other.

For the rest of the chapter, these two properties are called Property (a) and Property (b) respectively. The cyclic-shifting is in terms of frequency sub-channels and can also be illustrated by upward shifting of the matrix. Since no prior analysis has been done, we will evaluate and compare all forms of random codes to uncover those that give a better performance. The implementation issues of the corresponding encoders will also be discussed in this section.

6.3.1 Types of random Frequency-Time codes

We categorize the random FT codes into four main types based on presence of the above two properties. The codes types are labeled accordingly in Table 6.1. Examples of all types of FT code in this section will be presented with frequency diversity order $L = 2$, and time hop $H = 3$.

Table 6.1 Frequency-Time Code Types

	FT Codes			
	Type I	Type II	Type III	Type IVa & IVb
Properties (a)	No	Yes	No	Yes
Properties (b)	No	No	Yes	Yes

For Type I, it is the most randomized code without both properties (a) and (b). An example of such code is shown in Figure 6.3. In this type, the total weight of value

$L \cdot H$ is distributed, with equal probability, among all $N \cdot H$ number of entries. Since it is possible that a column in this code is without any weight, a hopping interval without any tone transmission on all sub-channels can exist.

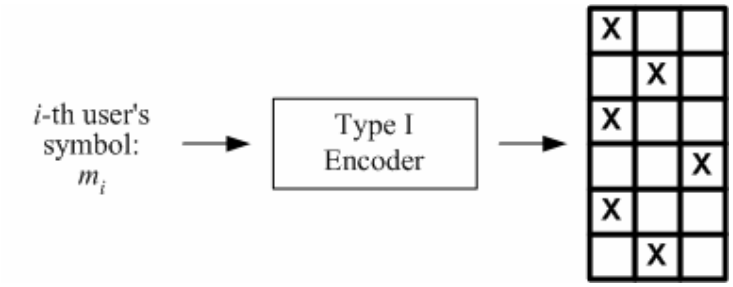

Fig. 6.3 Type I code

In Type II, the code has property (a) but not property (b). Its example is shown in Figure 6.4. Within each column of the code, L tones are distributed with equal probability among N number of entries. There are always L transmitting sub-channels at every hop.

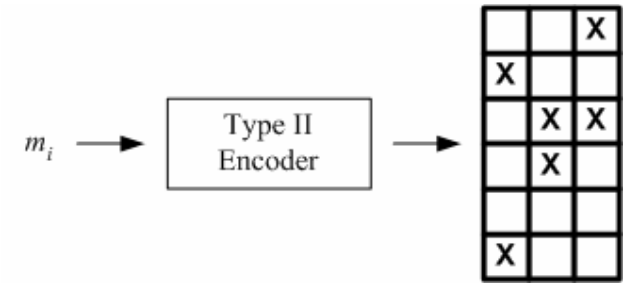

Fig. 6.4 Type II code

Type III code has property (b) but not property (a). When the FT codes assigned to the same user are cyclic-shifted versions of one another, they can be grouped and represented by a single address code/matrix instead. The encoding process will then consist of frequency-shifting a random address code by the symbol value m_i as shown in Figure 6.5.

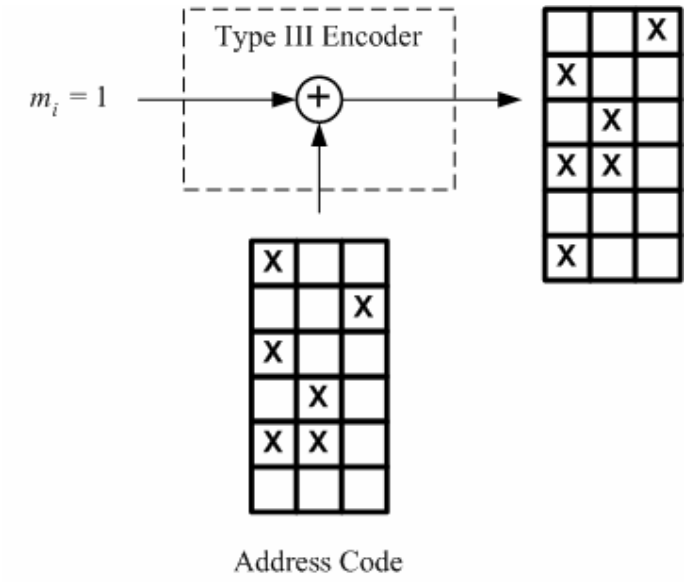

Fig. 6.5 Type III code

In Type IVa, the code has both properties (a) and (b). As in Type III code, an address code can be used to represent all the codes assigned to the same user. In addition, the weight of the address code must be equal to L at each column. The encoding process and an example of the code are shown in Figure 6.6. The encoding used in [15,16] belongs to this type. This encoding is also equivalent to an implementation of Sinha's MC-MFSK system [2], when the MC-MFSK signal is sent repetitively and a different address vector is used at each repetition.

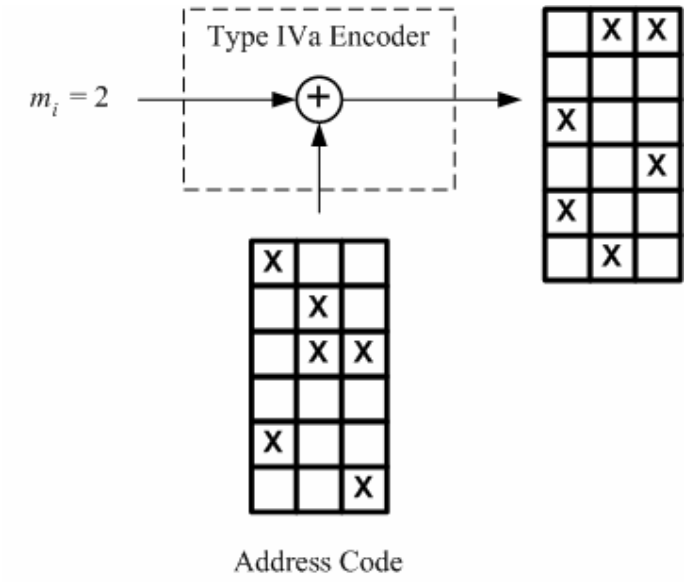

Fig. 6.6 Type IVa code

As for Type IVb code, it is a variant of the Type IVa code. Type IVb code not only has properties (a) and (b), but the columns of the codes are cyclic shifted versions of one another as well. An example of the code is shown in Figure 6.7. This encoding is equivalent to an implementation of the MC-MFSK system [2] with repetitive signaling as above. But the same address vector is used at each repetition and is further cyclic-shifted by a frequency hopping sequence. The encoding process is also shown in Figure 6.7.

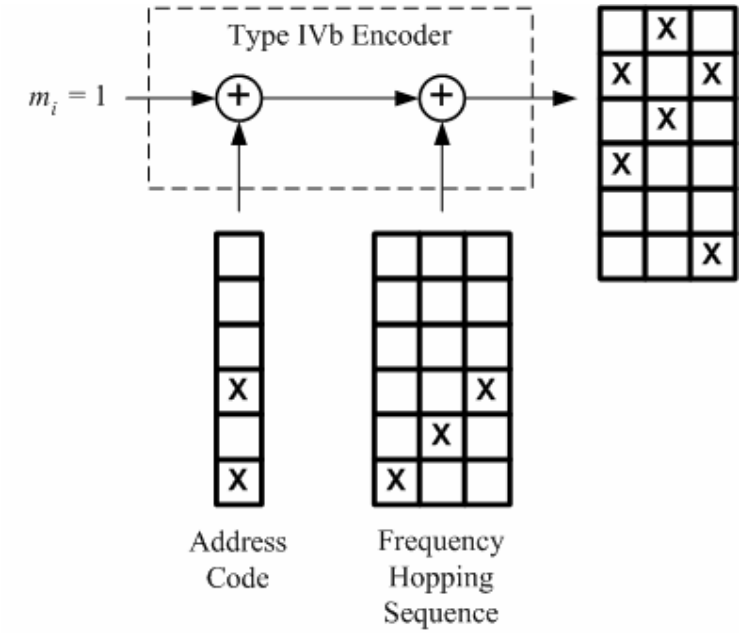

Fig. 6.7 Type IVb code

6.3.2 Performance of Codes

We now analyze the correlations of these codes and compare their performances. Two kinds of correlation are of concern here, the cross-correlation and auto-correlation. The former indicates the degree of interference with other user, while the latter indicates the degree of self-interference.

Cross-Correlation

Let random variables Y_a and $Y_{\bar{a}}$ denote the cross-correlation of codes with and without property (a) respectively. Codes without property (a) have all their $L{\cdot}H$ weights distributed evenly among the $N{\cdot}H$ entries. We assume that the occupancy among the entries in a code to be mutually independent. Hence $Y_{\bar{a}}$ is approximated to be a binomial distribution of $L{\cdot}H$ trials, each with L/N probability of being occupied.

We denote a binomial distribution with n trials and p probability of success as $\boldsymbol{B}(n, p)$, therefore the distribution of $Y_{\bar{a}}$ can be represented as $Y_{\bar{a}} \sim \boldsymbol{B}(HL, L/N)$.

As for Y_a, it is the sum of cross-correlation at each hop. Within each hop, L tones are distributed evenly among N entries, thus the correlation of each hop approximates to the binomial distribution $\boldsymbol{B}(L, L/N)$. For random codes, the correlations among the hops are independent. Therefore, the random variable Y_a is given by the sum of H independent random variables, each of binomial distribution with the same occupancy probability. Hence the distribution of Y_a can be represented as $Y_a \sim \boldsymbol{B}(HL, L/N)$.

Since Y_a and $Y_{\bar{a}}$ have the same distribution, we deduce that property (a) does not affect the cross-correlation of the codes. In addition, property (b) also does not affect the cross-correlation distribution, as the property is only applicable to codes assigned to the same user. Hence we conclude that the level of cross-correlation (thus the degree of external interference) is the same for all code types.

Auto-Correlation

For codes without property (b), a set of codes is randomly allocated to each user. Each code in the set is uniquely assigned to each of the M symbols from that user. These codes of the same user are independent, and correlations between them are equivalent to correlations with codes from other users. Hence the off-peak auto-correlation of Type I and II codes have the same distribution as the cross-correlation, and are given by $\boldsymbol{B}(HL,L/N)$

For codes with property (b) (Type III, IVa, IVb codes), only an address code is allocated to each user. Frequency cyclic-shifted versions of the same address code are assigned as codes to the symbols of that user. Therefore, these codes of the same user are not independent, and cannot be treated like cross-correlation. We denote $L_{h,i}$ and random variable Z_i as the number of tones and the off-peak auto-correlation of the ith hop respectively. Considering the total correlation over all erroneous cyclic-shifts within a hop, there is a total correlation of $L_{h,i}$ ($L_{h,i}$ -1) spread over $L_{h,i}$ (N -1) entries. Therefore Z_i has a binomial distribution, $Z_i \sim \boldsymbol{B}(L_{h,i}, \frac{L_{h,i}-1}{N-1})$. The auto-correlation of a code will be the sum of correlations in each hop Z_i.

For Type III code, since the number of tones in each hop is not necessary equal, the distributions of each Z_i's will also not have the same occupancy probability. The off-peak auto-correlation of this code will be a sum of H binomial distribution with unequal occupancy probability. Mathematically, the resulting distribution of the Type III auto-correlation will be given by $\sum_{i=1}^{H} Z_i$, where Z_i's are independent for all i and $\sum_{i=1}^{H} L_{h,i} = HL$.

As for Type IVa code, all hops have the same number of tones, $L_{h,i} = L$ for all i. The auto-correlation of Type IVa code will be sum of H binomial distributed Z_i's, where Z_i's are independent and have same occupancy probability $\frac{L-1}{N-1}$. Hence the auto-correlation of this code has distribution given by $\boldsymbol{B}(HL, L\text{-}1 / N\text{-}1)$.

In the case of Type IVb code, the columns of the FT code at every hop are cyclic-shifted version of the same vector. After they are de-hopped by the frequency hopping sequence, the columns of the FT code will be repetition of one another. On decoding, the auto-correlation at each hop will then be the same. Therefore, we drop the subscript in Z_i and denote the auto-correlation of each hop here as $Z_i = Z \sim B(L, \frac{L-1}{N-1}), \forall i$. The off-peak auto-correlation of the Type IVb code is then given by $H \cdot Z$.

Comparison of codes

We summarize the auto-correlation of each type in Table 6.2. We also show the mean and variance in Table 6.2, where $D = \frac{HL^2}{N}$, $D' = \frac{HL(L-1)}{N-1}$, $E = \frac{HL^2(N-L)}{N^2}$, and $E' = \frac{HL(L-1)(N-L)}{(N-1)^2}$. Note that $\frac{L-1}{N-1} \approx \frac{L}{N}$ and $\frac{L-1}{(N-1)^2} \approx \frac{L}{N^2}$ for typical value of L and N, therefore $D \approx D'$ and $E \approx E'$.

Table 6.2 Distribution, mean and variance of auto-correlation for all code types

Code Type	Distribution of Auto-correlation	Mean	Variance
I	$\boldsymbol{B}(HL, L/N)$	D	E
II	$\boldsymbol{B}(HL, L/N)$	D	E
III	$\sum_{i=1}^{H} Z_i,\ Z_i \sim \boldsymbol{B}(L_{h,i}, \frac{L_{h,i}-1}{N-1})$	$\frac{H}{N-1}\left(\frac{\sum_{i=1}^{H} L_{h,i}^2}{H} - L\right) + D'$	$\sum_{i=1}^{H} \frac{HL_{h,i}(L_{h,i}-1)(N-L_{h,i})}{(N-1)^2}$
IVa	$\boldsymbol{B}(HL, L\text{-}1\ /N\text{-}1\ )$	D'	E'
IVb	$H{\cdot}Z,\ Z \sim \boldsymbol{B}(L, \frac{L-1}{N-1})$	D'	$H \cdot E'$

Since all cross-correlations are independent and are of common distribution for all code types, we can compare the performance of the codes solely by analyzing their auto-correlations. The nature of the system is that the error performance is largely dependent on the value of the maximum correlation. Although most of the erroneous symbols can have low correlation value, the error performance will be poor as long there is one erroneous symbol with high correlation value. Hence a good code is one which has correlation distribution of low variance and mean. We shall identify the good codes by first eliminating the undesirable ones.

Type III is a bad code because it has greater mean auto-correlation than the rest by the term

$$T = \frac{H}{N-1}\left(\frac{\sum_{i=1}^{H} L_{h,i}^2}{H} - L \right). \tag{6.1}$$

Since $T \geq 0$, with equality only when all $L_{h,i}$ is equal to the average frequency diversity order L, therefore the system using Type III code will suffer a higher degree of self-interference.

Type IVb is also a bad code as it has a greater variance than the rest by a factor H. Its performance will deteriorate drastically as the number of hops increases. Figure 6.8 shows an instance of the Type IVb code auto-correlation compared with a Type I, II or IVa code. The side auto-correlation of the Type IVb code always take values in multiples of H, and often has a maximum value greater than those of other codes.

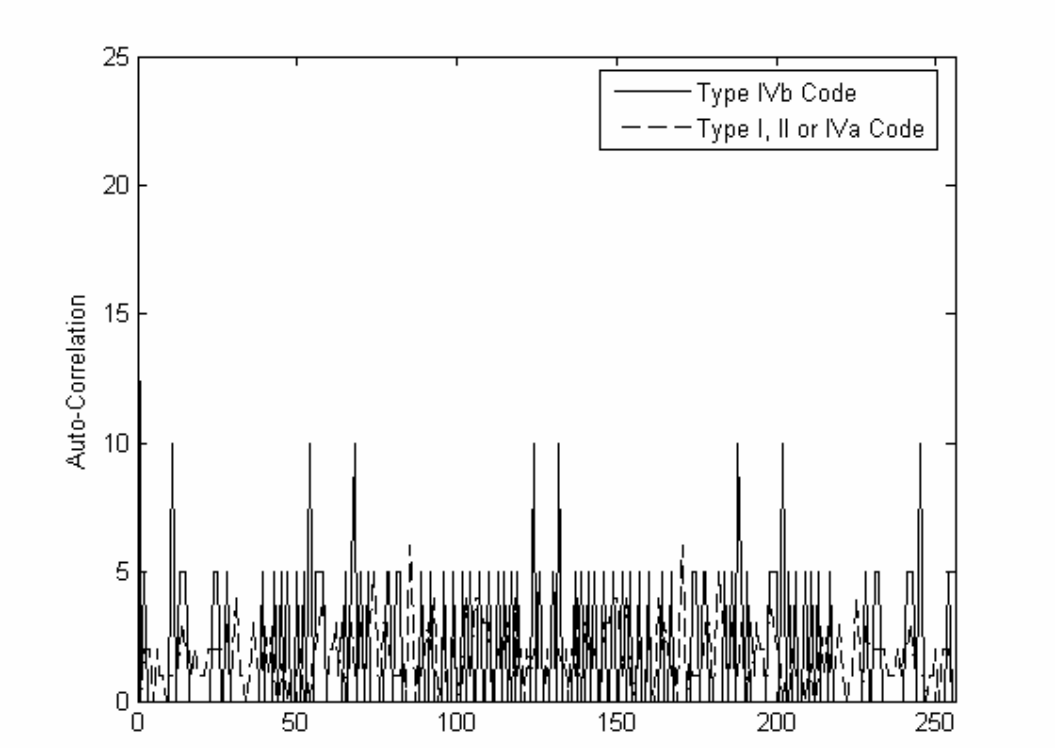

Fig. 6.8 Auto-correlation of FT codes with M=256, L=10, H=5

Hence out of the codes introduced, the good codes will be the remaining Type I, II and IVa codes. Since these three codes have similar auto-correlation distribution, they will also produce similar error performance in FHMC-MFSK systems.

6.3.3 Implementation Considerations of Codes

Depending on the possessed properties, the various code types will have different implementation considerations which we will discuss now. For codes without property (a) (Type I and III codes), the number of tones transmitted will change at each hop. The output power of the transmitter will then be irregular. There might also be a limit on the number of tones the transmitter can send in a hop, depending on the power limitation of the amplifier. However, with property (a), the size of the code is reduced.

For codes without property (b) (Type I and II codes), a multiplexer is required to map each symbol to the corresponding FT transmission. Memory is required to store the codes for every symbol. As for the rest with property (b) (Type III, IVa and IVb codes), the multiplexing of the transmission can be implemented by a frequency shift operation on an address code. In addition, only the address code of the users will have to be stored. However the sizes of these codes are reduced also for having property (b).

Although Type I, II and IVa codes produce the best performance equally, they all have different implementation considerations. Therefore the choice between these

three codes will depend on matching their considerations to the operation requirements.

6.4 Derivations and Optimization of Frequency Diversity Order

6.4.1 Derivation of Symbol Error Probability

In this section, we derive an analytical upper bound for the symbol error rate (SER) of FHMC-MFSK systems. This evaluation considers that the better-performing codes (Type I, II and IVa) are used, and where self-interference can be reasonably approximated as interference from an external user.

Unlike the complex evaluation provided by earlier studies [15,16], we derive a much simpler solution by using the same approach as in Chapter 3. Similar to the analysis in Chapter 3, we will assume that the system is a non-fading, AWGN channel with high SNR. The rationale is that since MAI has a more dominating effect on error performance than channel noise and fading, evaluation of error performance due only to it is sufficient. The effect of fading is curbed by the frequency and time diversity of the system and hence can be neglected. We will verify that our solution is still applicable to systems in fading channel for reasonable SNR.

In this system, each of the K simultaneous users transmits $L \cdot H$ tones equally distributed over $N \cdot H$ frequency-time slots. Taking that the codes are assigned randomly and with self-interference treated as external interference, the probability that an entry in $\boldsymbol{R}$ is occupied is given by

$$P_I = 1 - \left(1 - \frac{L}{N}\right)^K . \tag{6.2}$$

In practical systems, $L/N<<1$, and $K>>1$, hence we approximate P_I as

$$P_I = 1 - \exp\left(-\frac{LK}{N}\right). \tag{6.3}$$

Let P_{filled} denotes the probability that an erroneous row in $\boldsymbol{D}$ has all its $L \cdot H$ entries occupied. Approximating that the occupancy of each entry is mutually independent, we derived an upper-bound for P_{filled} as

$$P_{filled} \le \left[1 - \exp\left(-\frac{LK}{N}\right)\right]^{LH} . \tag{6.4}$$

With (M-1) erroneous symbols, a union bound for the symbol error probability P_e can then be formulated as

$$P_e \le \frac{1}{2}(M-1)\left[1 - \exp\left(-\frac{LK}{N}\right)\right]^{LH} , \tag{6.5}$$

where the factor ½ accounts for the random choice between the desired and the erroneous symbol.

Note that the SER in (6.5) is similar to our expression in (3.4) in Chapter 3 for the MC-MFSK system, except for the $L \cdot H$ exponential term. Hence by extending the MC-MFSK system (H=1) to the FHMC-MFSK system (H >1), we will improve the error performance exponentially.

The above analysis can be considered as an evaluation for the asymptotic performance at sufficiently large SNR. Therefore, it is also an upper bound for systems in fading channels at high SNR level. Our comparisons shows that (6.5) is valid for bounding performance at a reasonable bit SNR level of above 40 dB. An example is the comparison between our analytical SER upper-bound, and the simulation results of systems using Type IVa code in Rayleigh fading channels and operating at bit SNR = 40dB. The results are shown in Figure 6.9 and 6.10 for H=1 and H=2 respectively. In both cases, the analytical SER give a close bound of the simulation results. Note that an optimal L is observed at the minimum point of the error rate. This optimal point is closely predicted by the analytical solution, and will be evaluated in the later section.

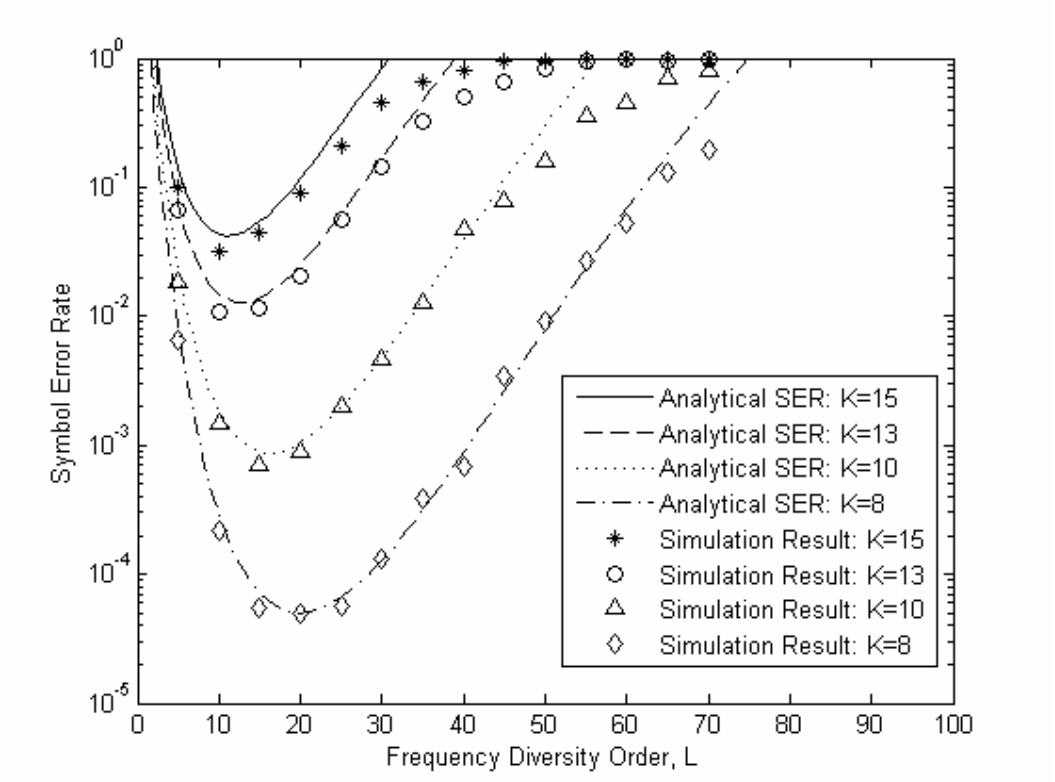

Fig. 6.9 Analytical and simulation SER for M=256, H=1, SNR= 40dB in Rayleigh channels

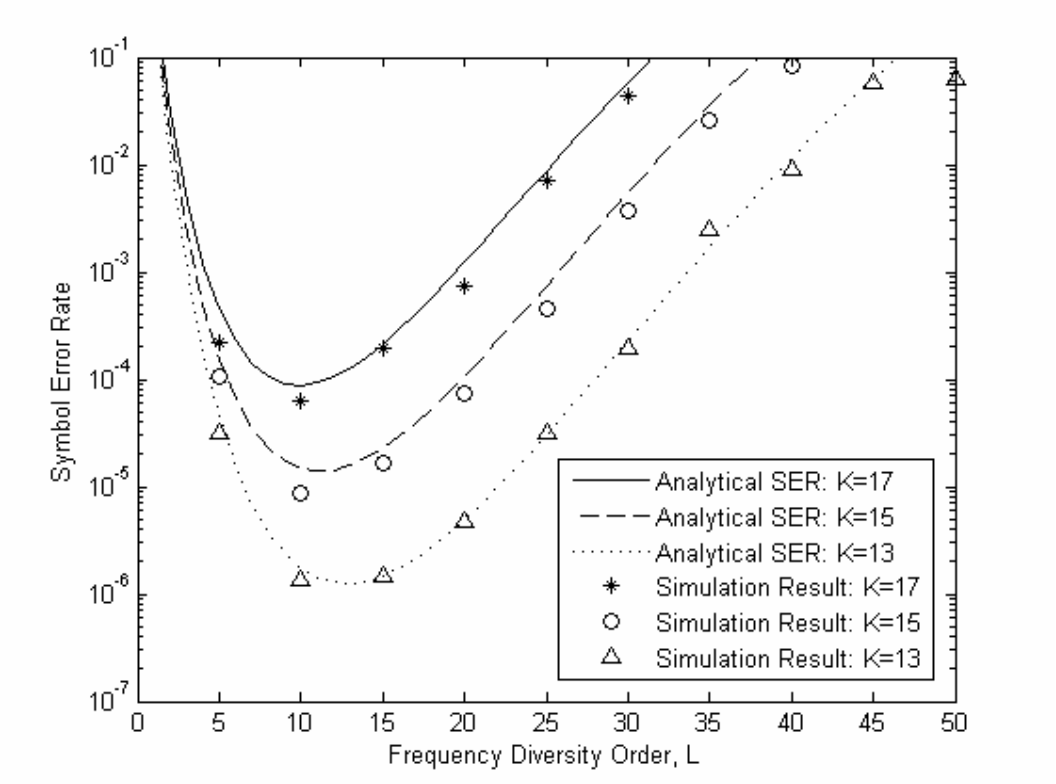

Fig. 6.10 Analytical and simulation SER for M=256, H=2, SNR= 40dB in Rayleigh channels

6.4.2 Derivation of System Bandwidth and Normalized Throughput

To preserve the orthogonality of the sub-channels, a frequency separation of $1/T_h$ has to be maintained between them. T_h here denotes the hop interval and is related to the symbol interval T_s, and bit rate R_b by

$$T_h = \frac{T_s}{H} = \frac{\log_2 M}{H R_b}. \tag{6.6}$$

For a total N sub-channels, the bandwidth of the FHMC-MFSK system is hence given as

$$B = N \Big/ T_h = \frac{NH}{\log_2 M} R_b. \tag{6.7}$$

Similar to the MC-MFSK system, the frequency diversity L is intrinsic to the system and does not affect the bandwidth. However, the bandwidth is a function of the number of time hops H and bandwidth will increase with H.

We denote C as the system capacity in nats per channel use. The system capacity of the FHMC-MFSK system is similar to the capacity of the multiple-access Frequency-Hopped MFSK system [17], and can be expressed as

$$C = P_e \ln(P_e) + (1 - P_e)\ln(1 - P_e) + \ln M - P_e \ln(M - 1). \tag{6.8}$$

For the normalized system throughput, it is defined as

$$W = \frac{KC}{BT_s}, \tag{6.9}$$

and expressed in units of nats per second per hertz. Substituting (6.7) in (6.9), we can simplify the throughput expression into

$$W = \frac{KC}{NH}. \tag{6.10}$$

6.4.3 Optimization of Frequency Diversity Level

Here we evaluate for an optimal L that will maximize the system throughput W. We can observe from (6.8) and (6.10) that W will vary inversely with P_e, when P_e is in a typical region ($P_e \le \frac{M-1}{M}$). Taking that the other parameters, K, N, H and M, are independent of L, the optimal L that maximizes W will minimize P_e as well,

$$\max_{L}\{W\} = \min_{L}\{Pe\}. \tag{6.11}$$

We then evaluate the optimal L by solving the first derivative of P_e in (6.5),

$$\frac{\partial P_e}{\partial L} = \frac{1}{2}(M-1)\left[1-\exp\left(-\frac{LK}{N}\right)\right]^{LH} H\left[\frac{\frac{LK}{N}\exp\left(-\frac{LK}{N}\right)}{1-\exp\left(-\frac{LK}{N}\right)} + \ln\left(1-\exp\left(-\frac{LK}{N}\right)\right)\right] = 0. \tag{6.12}$$

From (6.12) we yield the condition for the optimal frequency diversity as

$$L = \frac{N}{K}\ln 2. \tag{6.13}$$

Note that this solution is unaffected by the number of time hops, and is the same for both FHMC-MFSK and MC-MFSK systems.

6.5 Effects of System Parameters

In this section, we will study the effect of each of several parameters, number of time hops, frequency diversity order, number of sub-channels, and modulation level, on the system behavior and the system demands.

First is the number of time hops, also known as the time diversity, H. From (6.5), increase in H improves the SER exponentially. However, as seen from (6.7), it also multiplies the bandwidth requirement. Increase in time hops will increase the number of tones used to transmit a symbol. With more tones per symbol, the power in each

tone is reduced. This will degrade the performance of our multi-tone system in AWGN channel [6].

Next is the number of tones per hop, known also as the frequency diversity, L. A higher L can improve error performance by increasing the system diversity, but it also can degrade performance by increasing the degree of interference. The extent of each effect will depend on the code employed. For random codes, a balance is found on the optimal value for L as shown in (6.13). The L has no effect on the system bandwidth. However, it does directly affect the power division among the tones like H above, thus affects performance in AWGN channel.

In the case of the number of frequency sub-channels N, a greater number will improve the error rate and will increase the cardinality of the code. However, it will multiply the bandwidth requirement.

Lastly, on the modulation level M. A higher M will mean more symbols, and a higher demand on the code cardinality when the number of user is constant. The error performance will also degrade due to more erroneous symbols. However, as long that the code cardinality demand is satisfied, a higher M will increase the spectral efficiency. For a constant power per bit, a greater M increases the power of each tone, hence improving performance in AWGN channel.

6.6 Conclusion

We have analyzed the FHMC-MFSK system, which is an extension of the MC-MFSK system to include time diversity via frequency-hopping. Since Frequency-Time (FT)

codes are required in FHMC-MFSK systems to select the multiple sub-channels at different hop interval, an analysis of the various types of the random FT code is made. We identify the types of random FT code with good performance and present their corresponding implementation considerations. By choosing the better-performing codes and evaluating the system performance due solely to multiple access interference, we derive a simpler expression for the error probability of FHMC-MFSK systems than previous works in literatures. This expression is verified to closely upper-bound the simulation result of the system in Rayleigh fading channels for bit SNR above 40 dB. Our expression shows the exponential relationship between time diversity and the error performance. We also derive the expressions for the system bandwidth and throughput, thus highlighting the relationship of these measurements to the system parameters such as frequency diversity, and modulation level. We then find the optimal frequency diversity order for maximum throughput. Interestingly, the condition for optimal frequency diversity order is the same as the condition in MC-MFSK systems, and is independent of time diversity. Based on our results, we discuss the effects of all the system parameters on the FHMC-MFSK system in order to understand the system behavior. We conclude the FHMC-MFSK system a feasible frequency-hopping variant for the MC-MFSK system. Similar to the MC-MFSK system, the FHMC-MFSK system can be optimized for maximum performance by making use of the analysis in chapter 3.

Chapter 7

Conclusion

We have derived a new error probability formula for the MC-MFSK system in interference-limited and non-fading channels. This error formula is mathematically simpler than previously published results. By making use of this analytically tractable formula, for the first time we derive the expression for the optimal diversity order. Since the multiple-access-interference is the dominating factor at high SNR, our expression for optimal diversity is also applicable in fading channels at high SNR. We compare our newly derived optimal diversity with the numerically searched results from previous works, and verify that our expression is valid for both Rayleigh and Rician fading channels at a practical SNR of above 40dB. We also present the optimal solutions for diversity order and modulation level for the system when under several constraints such as the minimum error rate and restriction on number of user.

Next we analyze the MC-MFSK system for distributed control of the diversity order. By formulating the objective functions for cases of non-cooperative and cooperative users, we show that a steady state solution for the optimal diversity orders exists at each case. We also derive the formulas for these solutions. We present computation results based on these formulas and verify them using simulations. We have pointed out that these solutions for non-cooperative and cooperative users are significant as they represent respectively the Nash equilibrium point and Pareto efficient point in game theory. Base on our analytical results for the steady state diversity order for

non-cooperative case and cooperative case, we can further optimize this distributed-control MC-MFSK system by using the concepts of pricing [21].

We propose a method for sub-channels selection in MC-MFSK systems for the first time. The selections of sub-channels, based on Balanced Incomplete Block (BIB) design, are assigned to each symbol of every user. The selections are such that any two selections coincide at most in a single sub-channel. Hence the method reduces the degree of multiple-access interference, and improves the error performance. We derive the expressions for the error probability and user capacity of MC-MFSK systems using this method of sub-channels selection based on BIB design. These expressions show the optimal diversity order for maximum error performance, and the optimal modulation level for maximum user capacity. Based on the effect of these parameters, we also present a method in selecting optimal parameter pair for BIB design that will maximize error performance. We simulate the performance of MC-MFSK systems employing our sub-channels selection method and conventional MC-MFSK systems. Our simulations show that the proposed system does achieve a substantial improvement in error performance than conventional MC-MFSK systems. While this improvement is limited for only lower number of users, our results motivate further research for better codes/designs in sub-channels selection.

Also we extend the MC-MFSK system to the Frequency-Hopping Multi-carrier (FHMC)-MFSK system by introducing additional frequency-hopping to the MC-MFSK system. In FHMC-MFSK systems, various types of frequency-time code can be generated to select the multiple sub-channels at different time-hops. We select three types of frequency-time codes based on their superior correlation distribution,

and present their implementation issues. We derive an expression for the error probability of FHMC-MFSK systems by considering a interference-limited channel. Our analysis shows that the optimal frequency diversity order is the same for conventional MC-MFSK systems, and is unaffected by the number of time-hops. Although the number of time-hops increases the bandwidth requirement, it also improves the error performance exponentially.

We acquired more understanding on the relationships of various parameters that will achieve optimal performance. We have demonstrated the versatility of the MC-MFSK system by presenting various performance results on distributed diversity control, selection of sub-channels based on BIB design, and extension to frequency-hopping. We show how the maximum capability of MC-MFSK systems can be exploited in all these cases. With optimal choice of system parameters, the MC-MFSK system can achieve a better performance than previously considered in the literature.

References

[1] R. Sinha and R. D. Yates, "An OFDM Based Multicarrier MFSK System", In *Proc. IEEE-VTS Fall VTC 2000*, vol.1, pp.257-264, Sept 2000.

[2] R. Sinha and R. D. Yates, "Performance of Multicarrier MFSK in Fading Channels", In *Proc. IEEE-VTS Fall VTC 2001*, vol.3, pp. 1848-1851, Sept 2001.

[3] Z. Yu, C. C. Chai and T. T. Tjhung, "Performance Analysis of Multiple-Access Multicarrier MFSK Systems in Rician Fading", *IEEE WCNC*, vol.2, pp. 746-751, March 2003.

[4] S. B. Weinstein and P. M. Ebert, "Data transmission by frequency division multiplexing using the discrete fourier transform", *IEEE Trans. Commun.*, vol.19, pp. 628-634, October 1971.

[5] S. Verdu, *Multiuser Detection*, Cambridge University Press, 1998.

[6] G. E. Atkins and H. P. Corrales, "An Efficient Modulation/Coding Scheme for MFSK Systems on Bandwidth Constrained Channels", *IEEE J. Selected Areas Commun.*, vol.7, pp. 1396-1401, Dec 1989.

[7] M. Hall Jr., *Combinatorial Theory*, John Wiley and Sons, New York, 1986.

[8] F. G. McWilliams and N. J. Sloane, *The Theory of Error Correcting Codes*, North-Holland Pub. Co., Amsterdam, 1977.

[9] D. J. Goodman, P. S. Henry and V. K. Prabhu, "Frequency-Hopping Multilevel MFSK for Mobile Radio", *Bell Syst. Tech. J.*, vol.59, pp. 1257-1275, Sept 1980.

[10] E. A. Geraniotis and M. B. Pursley, "Error probabilities for slow frequency hopped spread-spectrum multiple access communications over fading channels", *IEEE Trans. Commun.*, vol.30, pp. 996-1099, May 1982.

[11] E. A. Geraniotis, “Multiple access capability of frequency hopped spread-spectrum revisited: An exact analysis of the effect of unequal power levels”, *IEEE Trans. Commun.*, vol.38, pp. 1066-1077, July 1990.

[12] K. Cheun and W. E. Stark, “Probability of error in frequency-hop spread-spectrum multiple-access communication systems with noncoherent reception”, *IEEE Trans. Commun.*, vol.39, pp. 1400-1410, Sept 1991.

[13] U.-C. Fiebig, “On the efficiency of fast frequency hopping multiple-access systems”, *IEEE ICC*, vol.1, pp. 33-37, June 1992.

[14] U.-C. Fiebig, “On the potential of FFH/MFSK CDMA for mobile radio systems”, *IEEE ISSSTA*, vol.1, pp. 332-337, Sept 1998.

[15] U. Timor, “Multitone Frequency-Hopped MFSK System for Mobile Radio”, *Bell Syst. Tech. J.*, vol.61, pp. 3007-3017, Dec 1982.

[16] T. Mabuchi, R. Kohno and H. Imai, “Multihopping & Decoding of Error-Correcting Code for MFSK/FH-SSMA Systems”, *IEEE ISSSTA*, pp. 199-202, Dec 1992.

[17] J. G. Goh and S.V. Maric, “The Capacities of Frequency-Hopped Code-Division Multiple-Access Channels”, *IEEE Trans. on Information Theory.*, vol.44, pp. 1204-1211, May 1998.

[18] H. S. Tay, C. C. Chai and T. T. Tjhung, “Optimal Diversity Order for Multiple Access Multi-Carrier MFSK Systems”, *paper in preparation for submission.*

[19] H. S. Tay, C. C. Chai and T. T. Tjhung, “Diversity Control in Multiple Access Multi-Carrier MFSK Systems”, *paper in preparation for submission.*

[20] A. B. MacKenzie and S. B. Wicker, “Game Theory in Communications: Motivation, Explanation, and Application to Power Control”, *IEEE GLOBECOM*, vol.2, pp. 821-826, Nov 2001.

[21] V. Shah, N. B. Mandayam and D. J. Goodman, “Power Control for Wireless Data based on Utility and Pricing”, *IEEE PIMRC*, vol.3, pp. 1427-1432, Sept 1998.

[22] J.G. Proakis, *Digital Communications*, McGraw-Hill, Fourth ed., 2001.

[23] M. Azizoglu, J. A. Salehi and Y. Li, “Optical CDMA via Temporal Codes”, *IEEE Trans. Commum.*, vol.40, pp. 1162-1170, July 1992.

[24] H. S. Tay, C. C. Chai and T. T. Tjhung, “Balanced Incomplete Block Design to Improve Performance of Multi-Carrier MFSK Systems”, *paper in preparation for submission.*